GRB observations to probe the evolution of the early Universe

Anatoly Iyudin
Extreme Universe Laboratory,
Skobeltsyn Institute of Nuclear Physics,
Moscow State University by M.V. Lomonosov

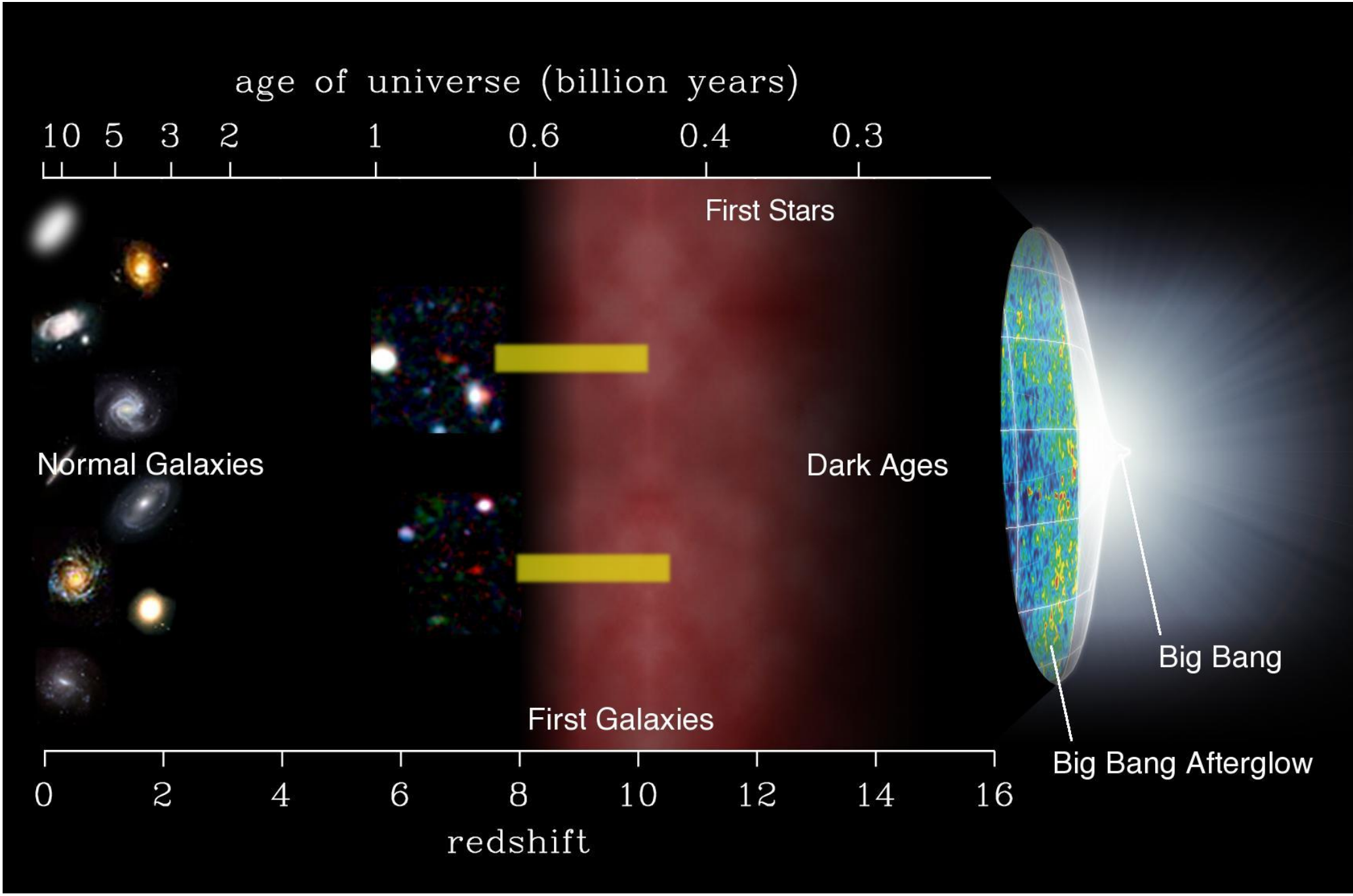
age of universe (billion years)
10 5 3 2 1 0.6 0.4 0.3
First Stars
Normal Galaxies
Dark Ages
Big Bang
First Galaxies
Big Bang Afterglow
0 2 4 6 8 10 12 14 16
redshift

Re-ionization history

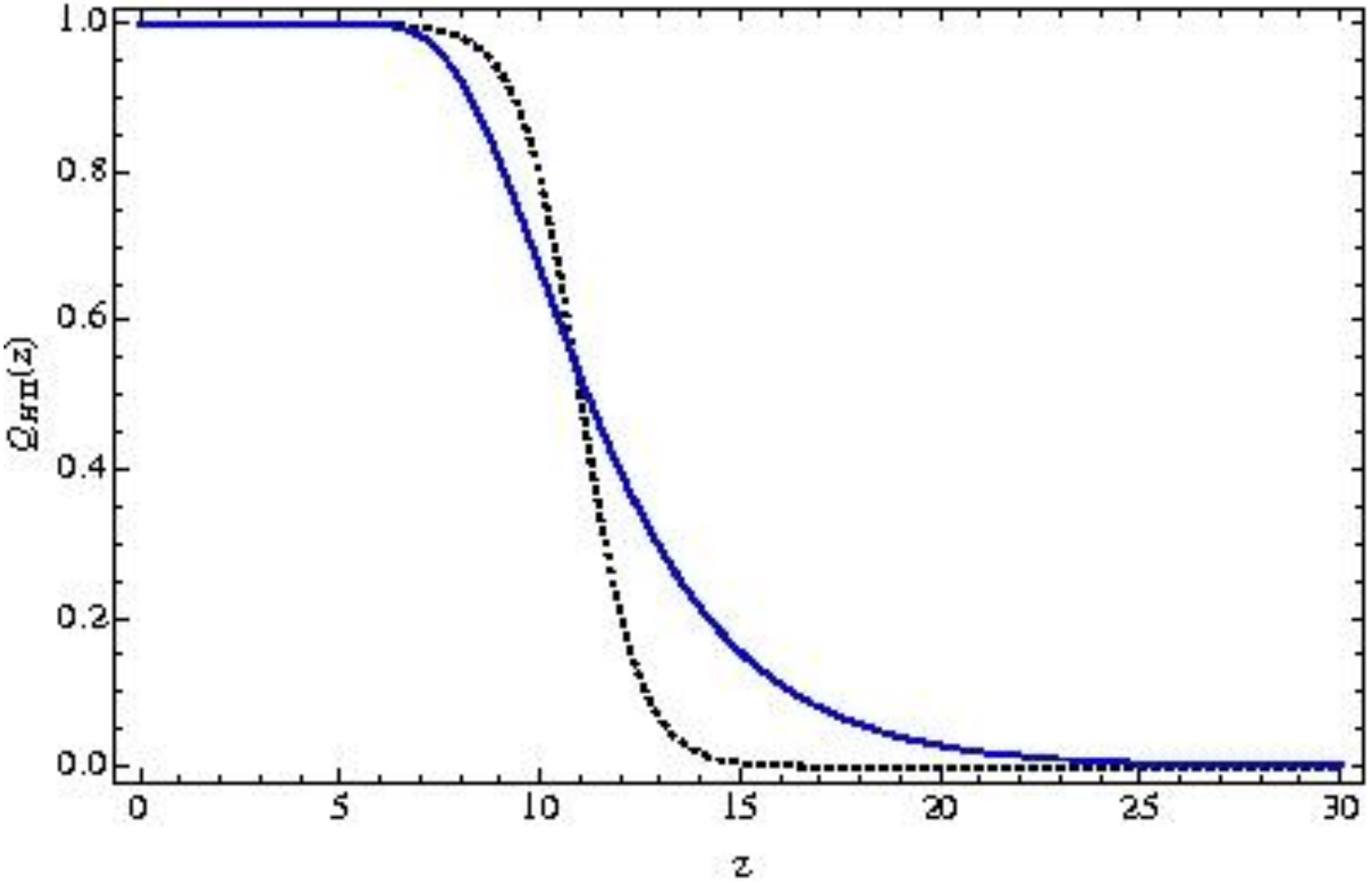

Re-ionization history calculated by de Souza, Yoshida & Ioka (2011). Blue line is model proposed by de Souza et al. (2011), while black dotted line is a result of calculation by using code CAMB, developed by Antony Lewis & Anthony Challinor (http://camb.info).

Understanding the early Universe

One of the most compelling problems facing modern astrophysics in 21-st century is to understand the early Universe, the epoch nicknamed as the Cosmic Dawn (Blandford et al. 2010).

Cosmic Dawn is the epoch when starlight from the first generation of stars start to ionize again the neutral intergalactic medium, and when the first objects of Universe start to form the structure which is prevailing until present.

Looking back in the time, this re-ionization was completed around the redshift of z~6 (Fan et al. 2006).

Understanding the early Universe

Potential probes of the Cosmic Dawn, include high-z quasars, galaxies and gamma-ray bursts (GRBs).

Normal galaxies can be found at very high redshifts (Bouwens et al. 2010) in the Hubble Ultra Deep Field through their photometric dropouts.

But these dropouts are not reliable, because they can be produced by the dust extinction.

Additionally, those galaxies represent the bright end of the luminosity distribution, but still are so faint, that it makes their spectroscopy unreliable, largely beyond the capabilities of existing instruments.

Understanding the early Universe

Potential probes of the Cosmic Dawn, include high-z quasars, galaxies and gamma-ray bursts (GRBs).

Each of these potential probes of the Cosmic Dawn, have their strong pro- and contra-points.

Quasars are extremely luminous and can be bright sources even at high redshifts, but the high UV and X-ray flux from the central engine strongly affects the properties of the host galaxy, making it atypical.

Moreover, density of quasars drops rapidly after z~6.

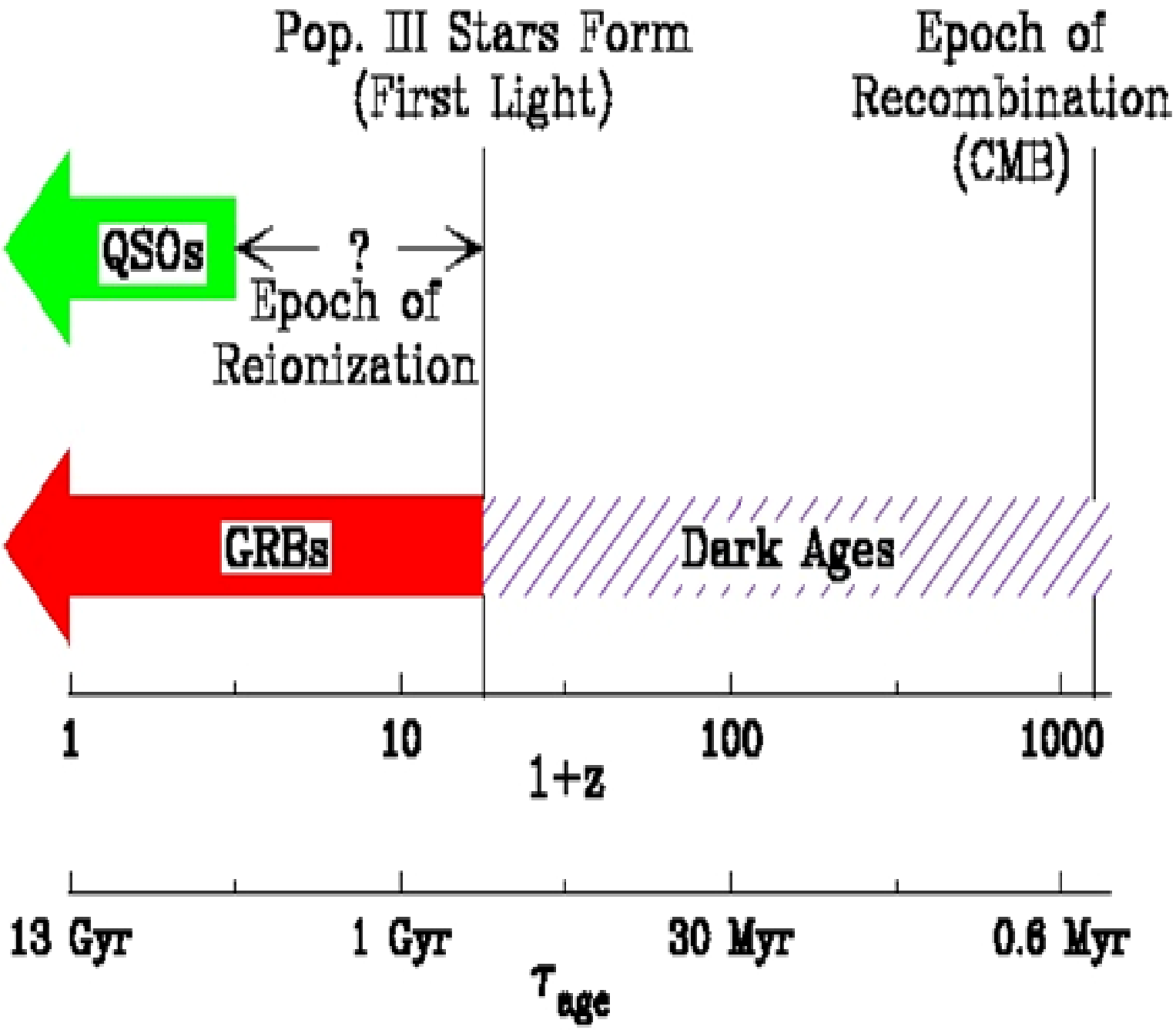

Lamb & Reichart 2000)

Understanding the early Universe

GRBs probe star formation regions in all types of galaxies,
are intrinsically bright, that can be used to probe the interstellar gas and dust
of host galaxies, even those that are very faint themselves.

The first stars in the Universe are thought to play a crucial role in the early cosmic evolution, by emitting first light and producing the first heavy elements (Bromm et al. 2009).

The standard cosmological model predicts that the first stars were formed when the age of the Universe was less than a few million years, and that they were predominantly massive (Abel et al. 2002; Omukai & Palla 2003; Yoshida et al. 2006).

There has not been yet a single direct observation of these first massive stars of the so-called Population III (Pop III). Recently it was proposed that massive PopIII stars may produce gamma-ray bursts, whose total isotropic energy could be $E_{iso} \geq 10^{55\text{-}57}$ ergs, i.e., ≥ 2 orders of magnitude larger than average (Komissarov & Barkov 2010; Toma et al. 2010; Meszaros & Rees 2010; Barkov 2010; Suwa & Ioka 2011).

Even if the PopIII stars have a supergiant hydrogen envelope, the GRB jet can break out the first stars because of the long-lasting accretion of the envelope itself (Suwa & Ioka 2011; Nagakura et al. 2011).

Observations of such energetic GRBs at very high redshifts will provide a unique probe of the young Universe.

Redshift distribution of potential probes

Yueksel +08 [arXiv:0804.4008v2]

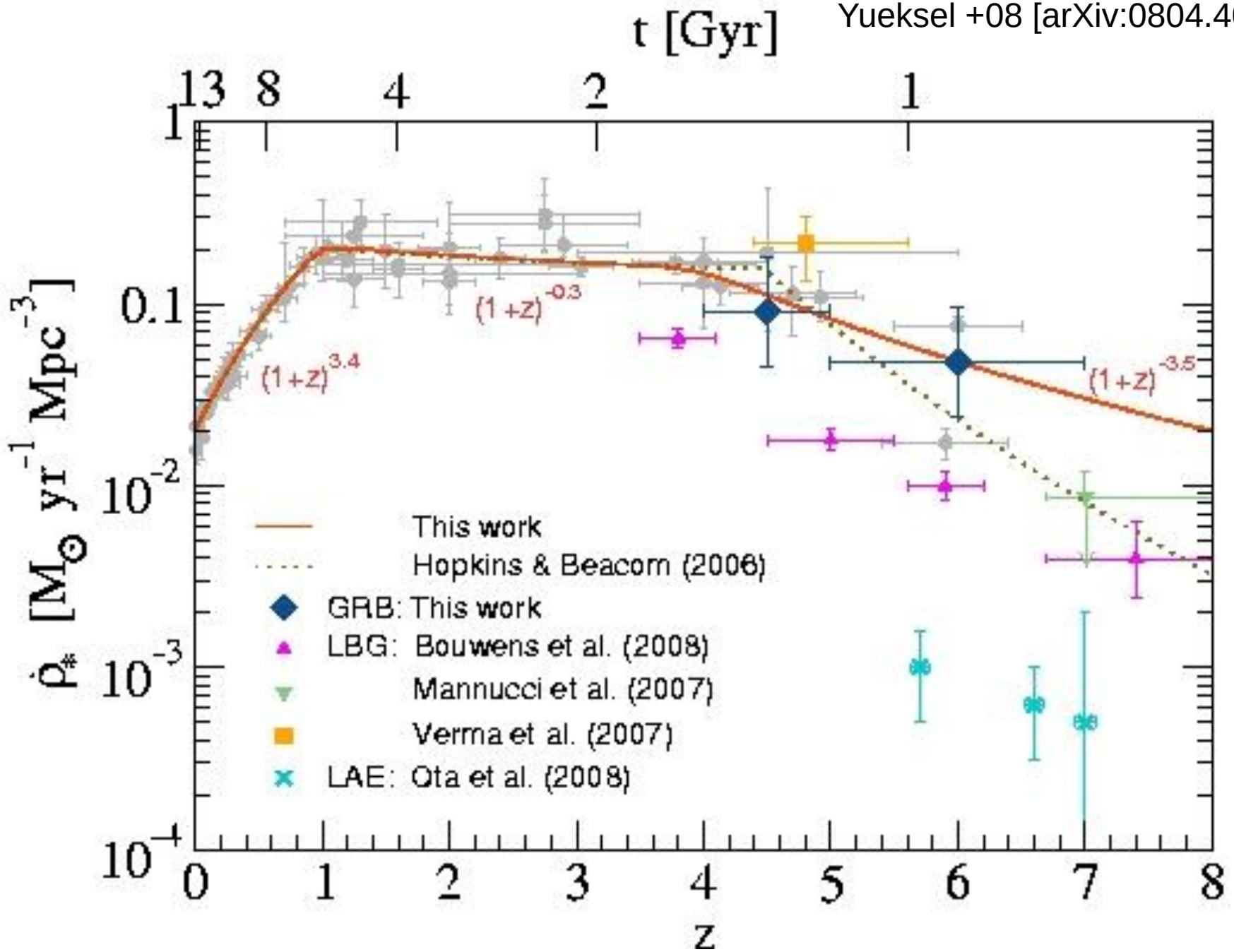

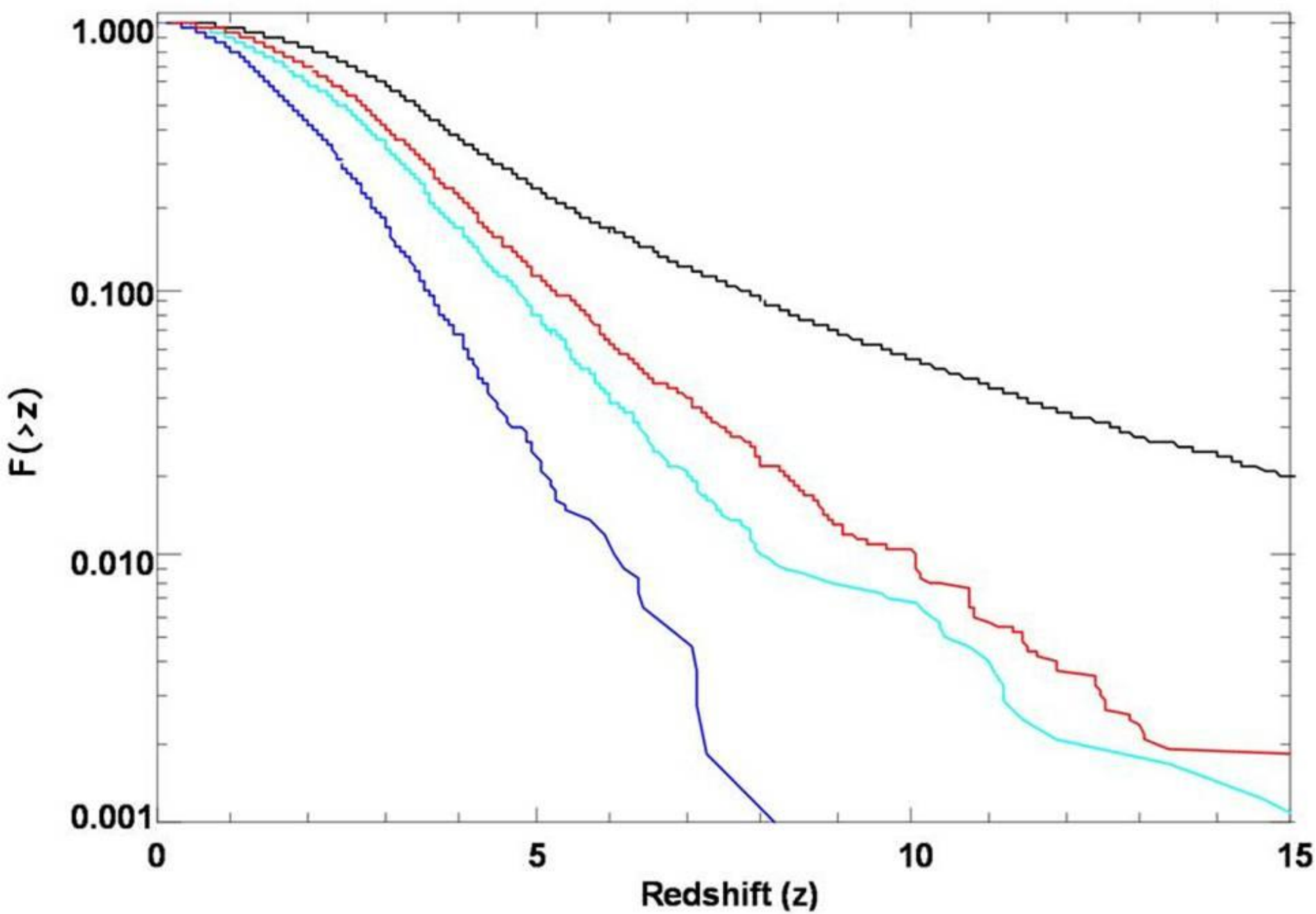

Redshift distribution of GRBs. The black line shows distribution of the parent population from Wanderman & Piran (2010). The cyan line shows the distribution for the *Swift* Bat instrument. The dark blue line shows the distribution for BATSE. The red line is for XCAT (*JANUS*, Burrows et al. (2012))

History of redshift-records

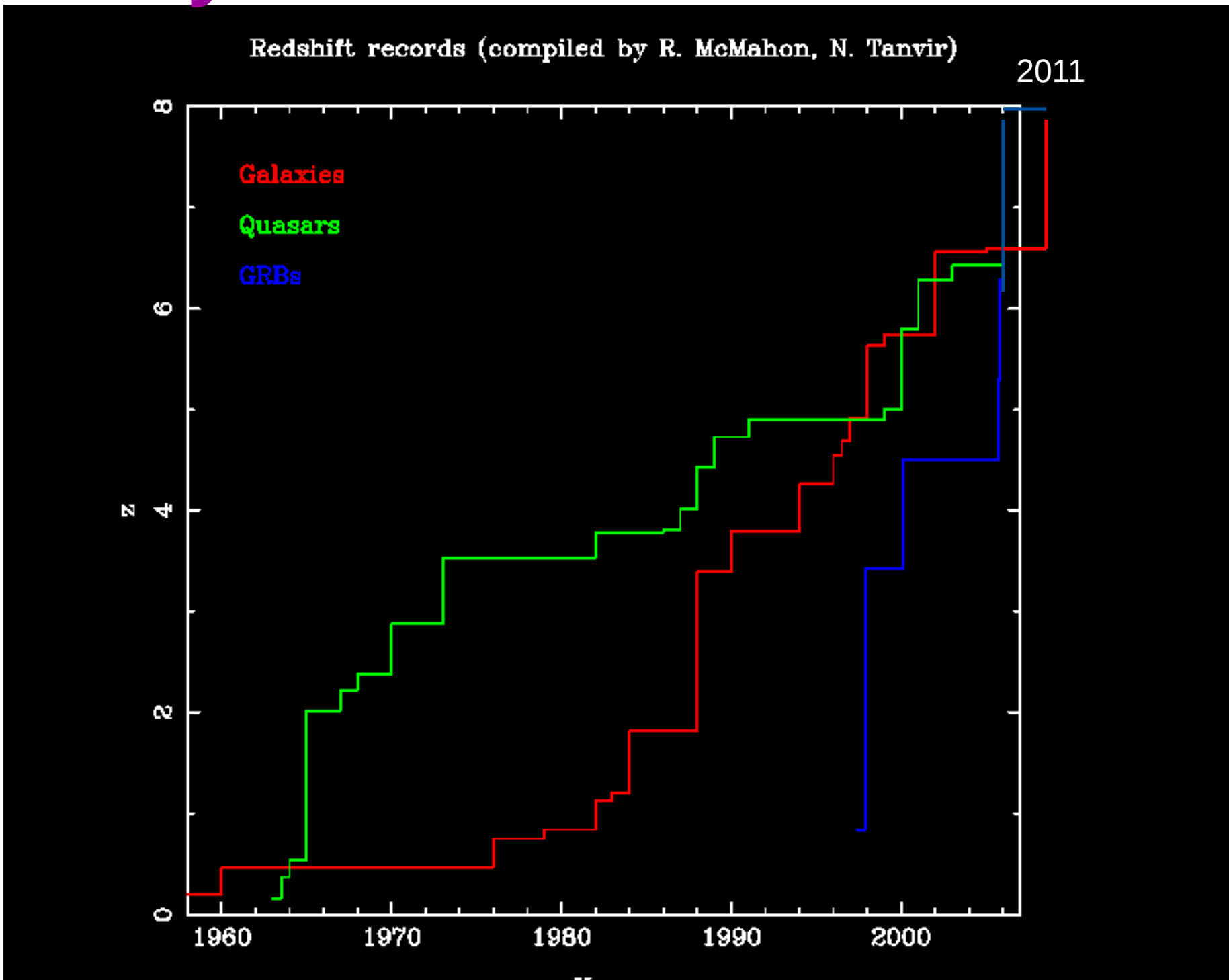

LDGRBs as a distance indicators

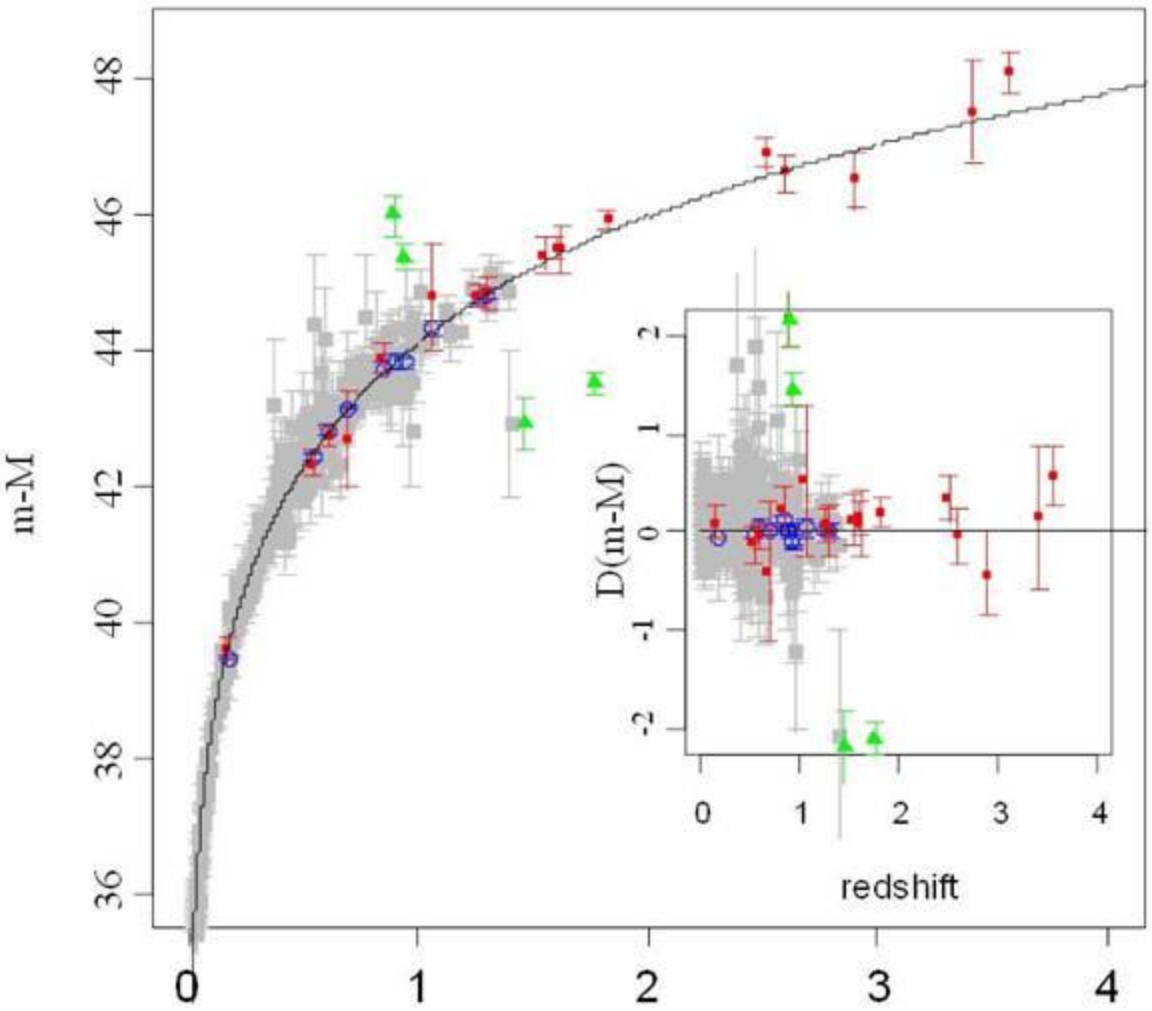

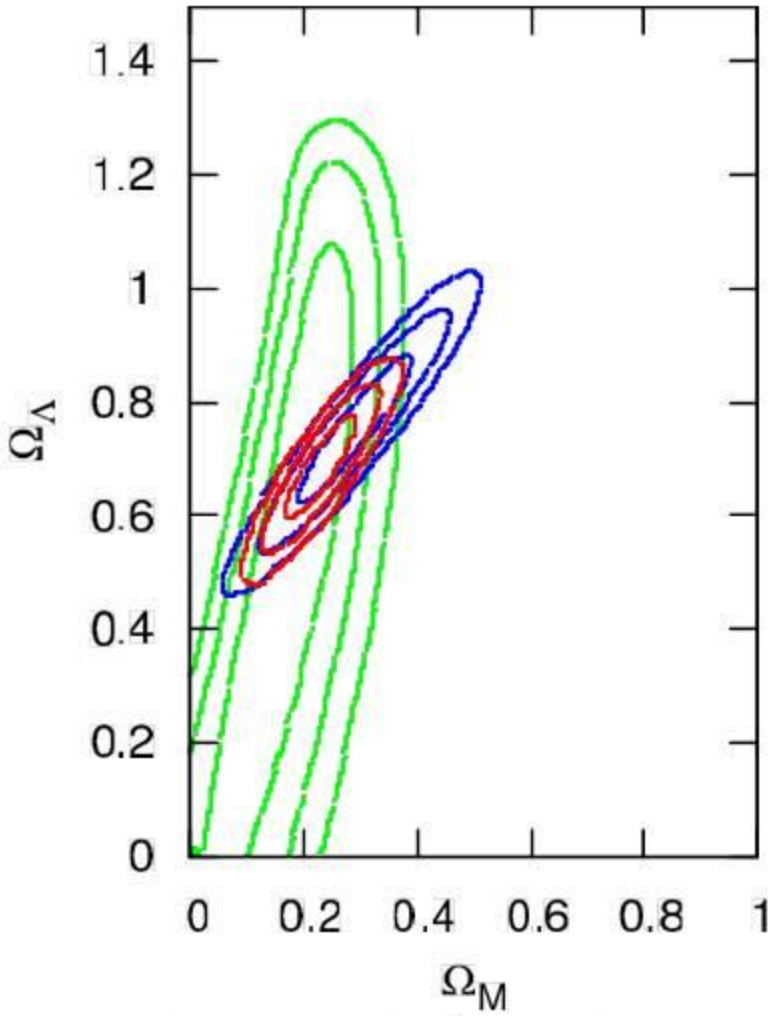

Tsutsui+2012, arXiv:1234.5678, See also: Liang, Wu, Zhang, PhRevD81, 083518(2010)

	Ω_M	Ω_Λ	χ^2/d.o.f
9 LGRBs (flat)	0.22 ± 0.04	-	5.09/7
557 SNe Ia (non-flat)	0.29 ± 0.10	0.76 ± 0.13	542.1/555
Combined (non-flat)	0.23 ± 0.06	0.68 ± 0.08	548.3/564

Table 3. Constraints on $(\Omega_M, \Omega_\Lambda)$ for flat universe from 9 LGRBs and for non-flat universe from 557 SNe Ia and 9 LGRBs + 557 SNe Ia with their reduced chi squares. All the quoted errors are at the 1-σ confidence level.

LDGRBs as a distance indicators

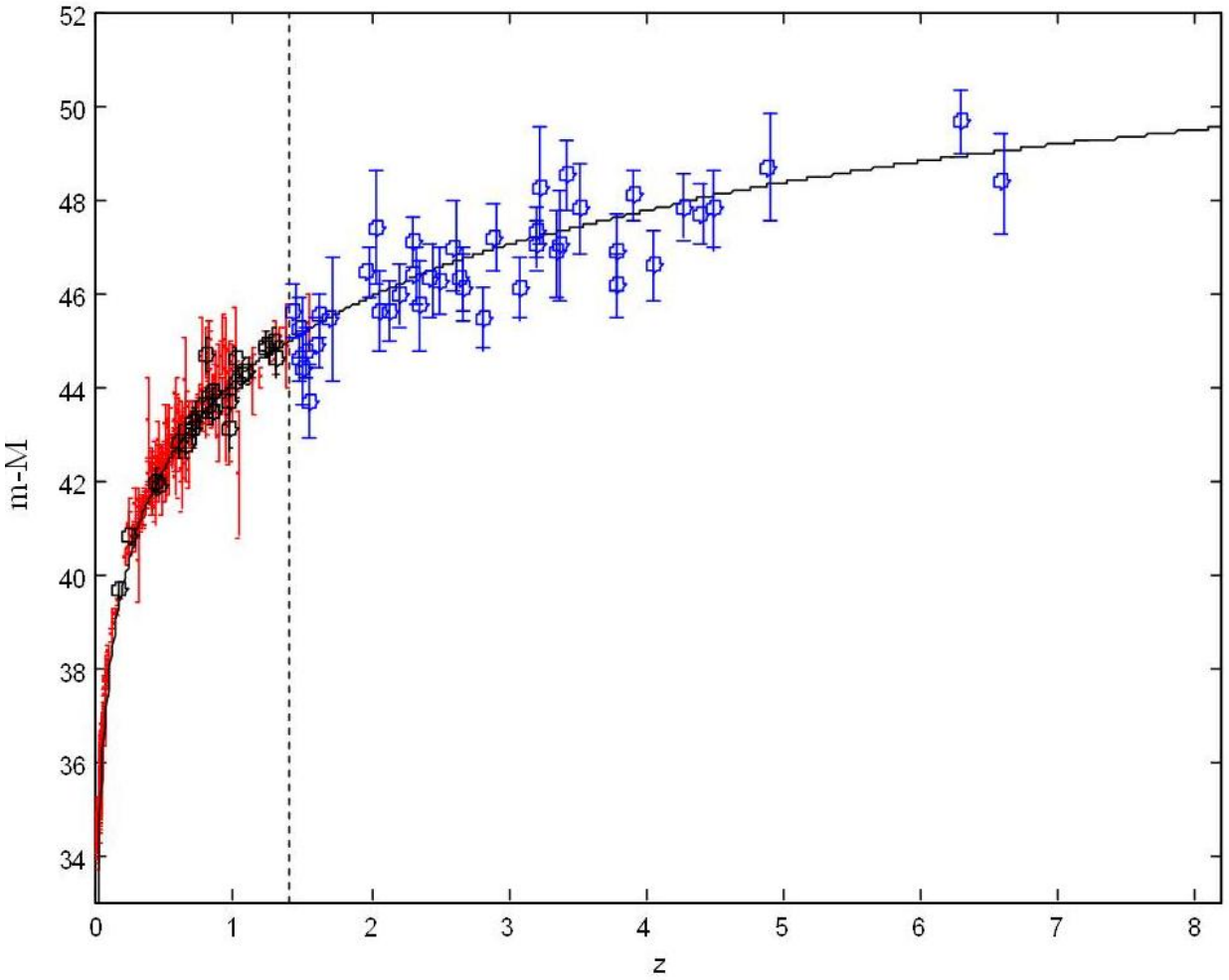

Liang, Wu, Zhang, Phys. Rev. vol. D81, 083518 (2010)

Hubble diagram of 397 SNIa (red dots) and the 69 GRBs (circles) obtained using the interpolation methods. The curve is the theoretical distance modulus in the concordance model (w= -1, $\Omega_{Mo} = 0.27$, $\Omega_{\Lambda} = 0.73$)

How to identify a high-z object?!

GRBs offer a promising opportunity to identify high-z objects, and moreover allow us to investigate the host galaxies at high redshift (z>10).

GRBs are a factor of 10^{5-7} brighter than quasars during the first hour after explosion, and their relativistic **k**-correction implies that they do not get fainter beyond z~3.

Present and near-future ground- and space-based facilities sensitivity limits the measurement of the redshift beyond z~ 13
(as H-band drop-outs), because GRB afterglows above 2.5 μm are too faint by many magnitudes for 8-10 m telescopes.

Afterglows and redshifts

(Slide is a courtesy of Thomas Kruehler)

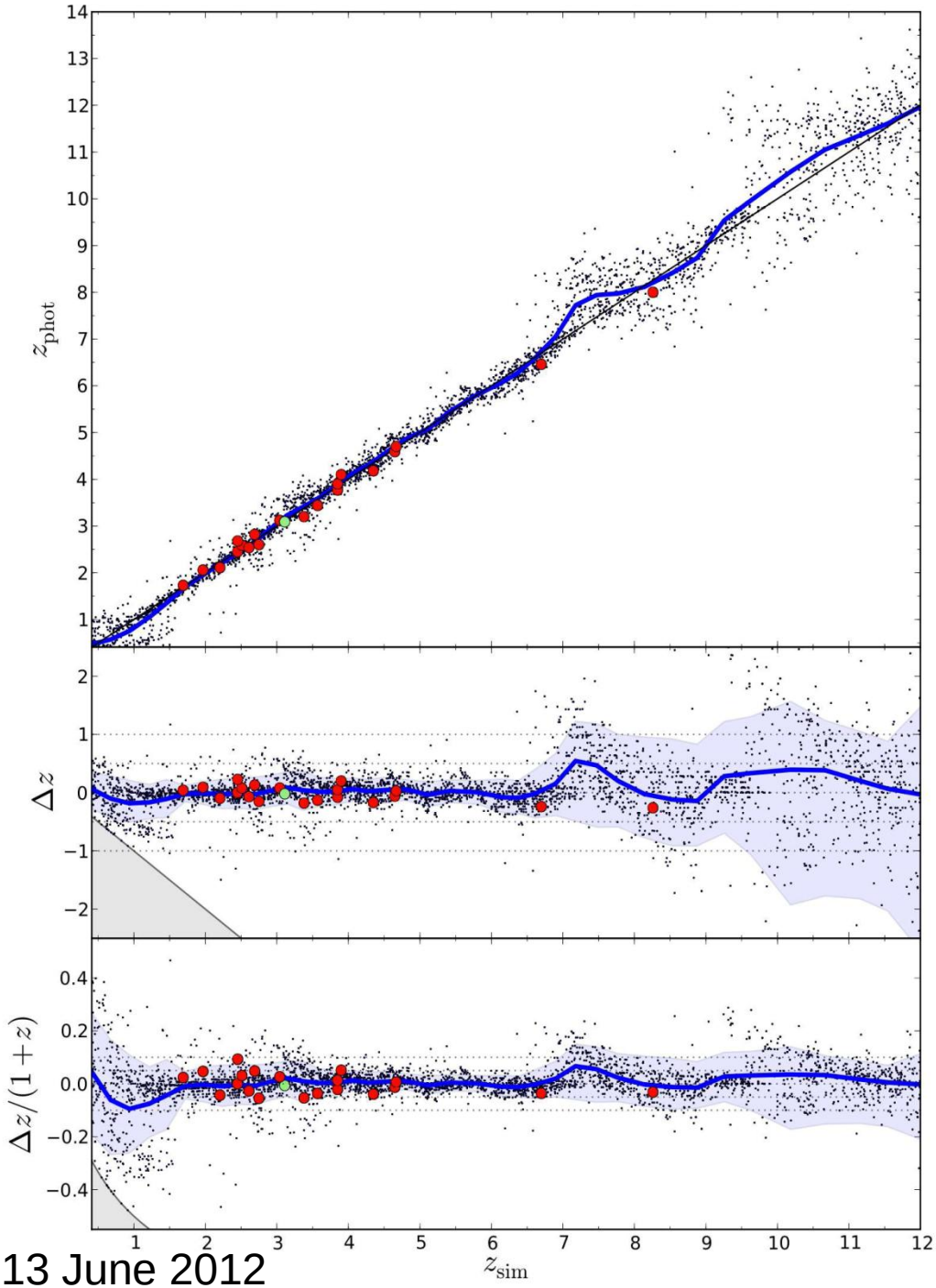

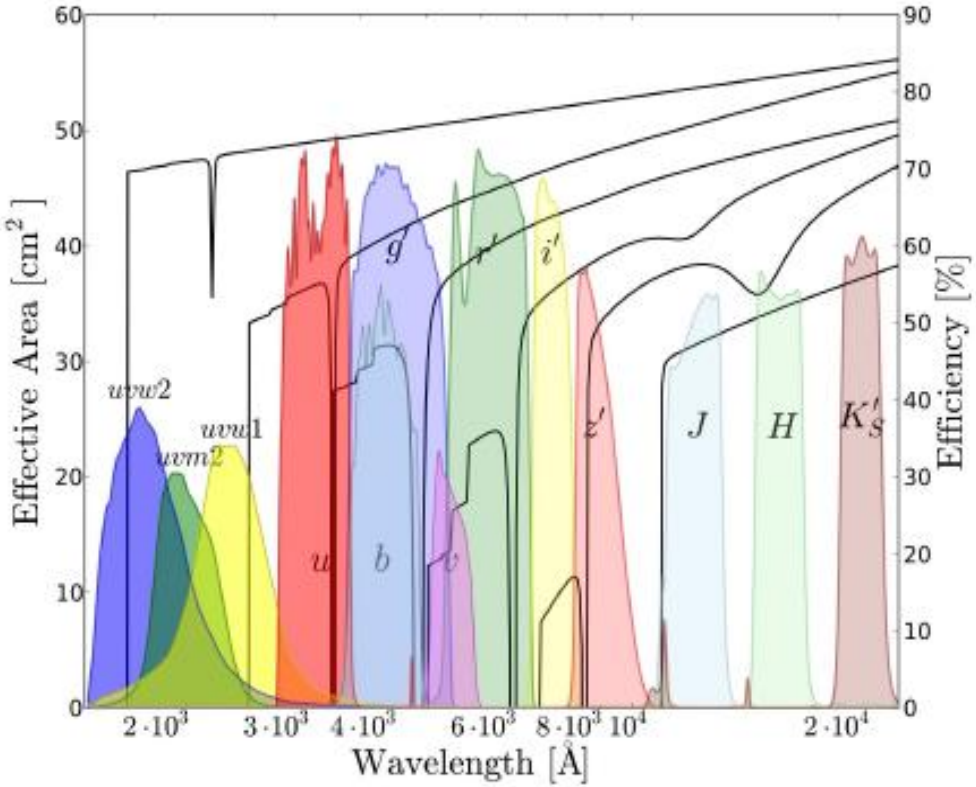

- Very good and robust photo-z's up to z ~ 10
- Simple spectrum
- Unique identification

Th. Kruehler+ 11

Afterglows and redshifts

(Slide is a courtesy of Thomas Kruehler)

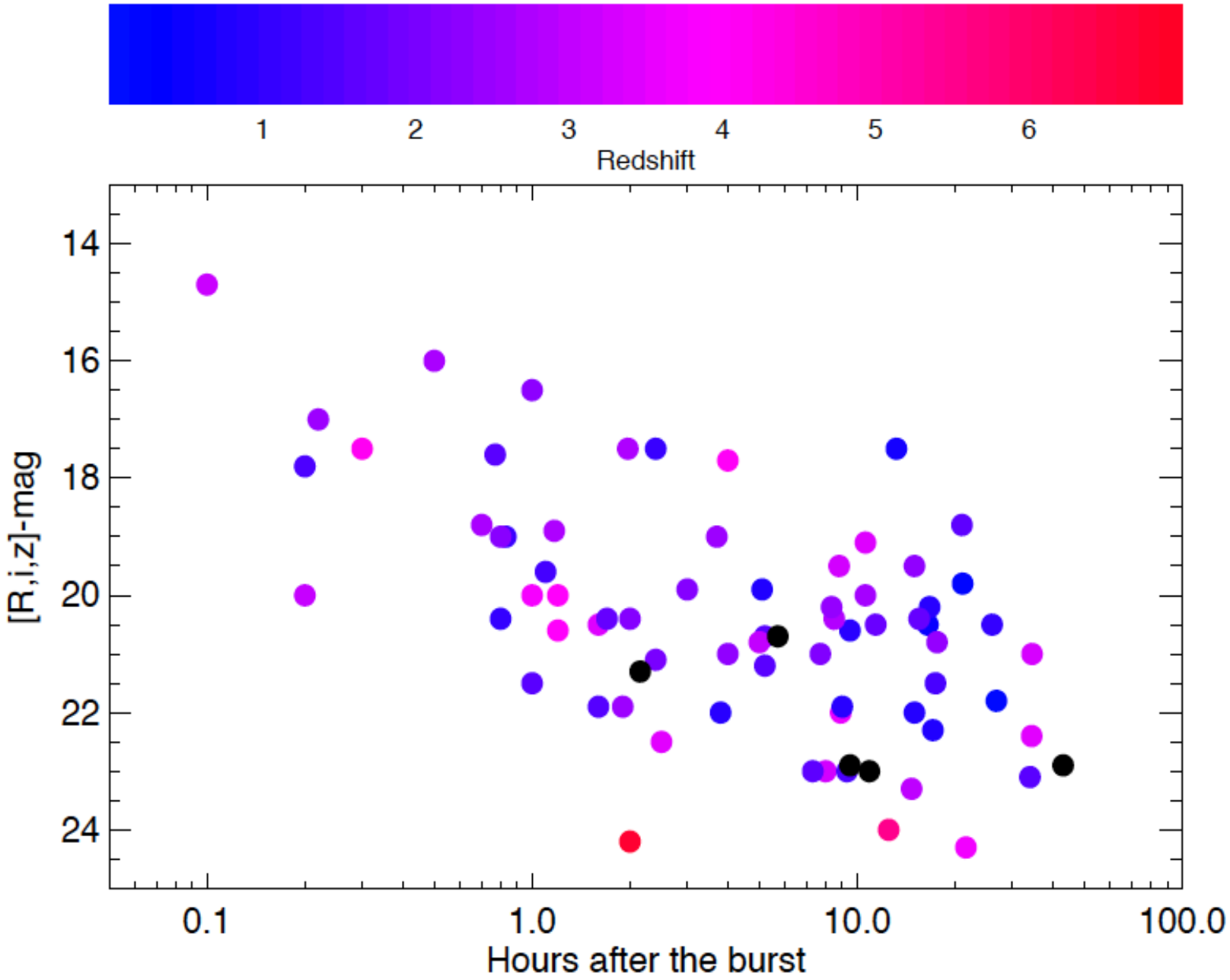

Fynbo+ 09

How to identify a high-z object?!

The use of GRBs as probes of distant galaxies has boomed since the launch of the Swift satellite (Gehrels et al. 2004), which is capable to provide rapidly positions of GRBs with a positioning accuracy on the order of arcseconds.

But, after six years of operation, Swift has found only 5 GRBs with the spectroscopic or photometric redshift exceeding z~6.

The paucity of the high-redshift GRBs found by Swift probably stems from several factors, with one of those being the long delay (typically a few hours) which is needed to obtain the first indication of GRB being a high-redshift event!

(see Table 1 from Burrows et al. (2011))

Table 1. Time delays to obtain redshift measurements for high-z *Swift* GRBs

GRB	z	Type[a]	T_P	T_S	References
050904	6.295	S	10 hr	3.5 days	Cusumano et al. (2006); Tagliaferri et al. (2005), Kawai et al. (2006)
060116	6.6	P	41 hr	N/A	GCN Circ. 4545
080913	6.695	S	10 hr	11 hr	Greiner et al. (2009)
090423	8.2	S	7 hr	24 hr	Tanvir et al. (2009)
090429B	9.4	P	2.5 hr	N/A	Cucchiara et al. (2011)

[a]P = photometric redshift, S = spectroscopic redshift
T_P = delay time to obtain photometric redshift; T_S = delay time to obtain spectroscopic redshift

To overcome this obstacle one can use a NRA signature in the SED of LDGRB (see Iyudin+ ’05, ‘08; Greiner+’09)

GRBs as light beacons

- GRBs follow the star formation rate
- Swift GRBs/afterglows can be seen up to z~20
- 5-50% of all GRBs are at z>5 (5% of Swift GRBs).
- GRBs are ideal light beacons to study early universe
  - Bright
  - Little affected by dust extinction
  - Simple spectrum (power law)
  - No pre-GRB ionization of surrounding

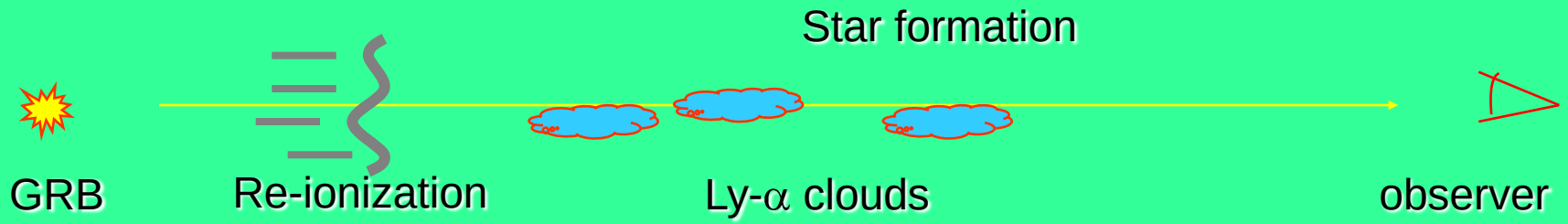

This artist's impression shows two galaxies in the early Universe. The brilliant explosion on the left is a gamma-ray burst. The light from the burst travels through both galaxies on its way to Earth (outside the frame to the right). Analysis of observations of the light from this gamma-ray burst made using ESO's Very Large Telescope have shown that these two galaxies are remarkably rich in heavier chemical elements. (Image courtesy: ESO/L. Calçada)

GRB 050904

Kawai et al. 2005

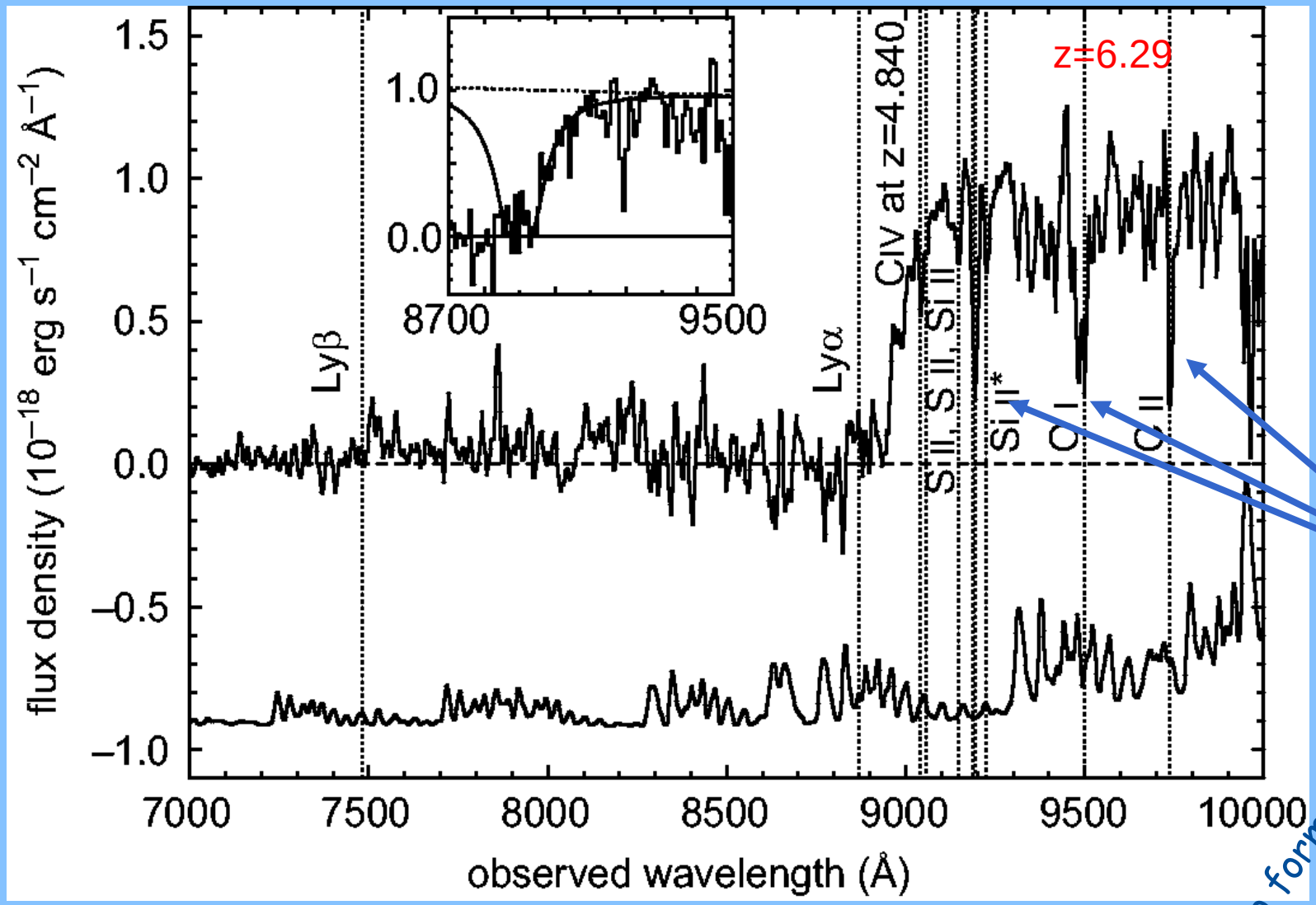

But how to form so much metals?

How to find high-redshift GRBs?

Due to characteristic spectrum of GRB Afterglow:

- Photometry in optical: up to z~6
- Photometry in NIR: up to z~12-14
- Beyond z~14: not feasible from ground ➔ in gamma-rays?!

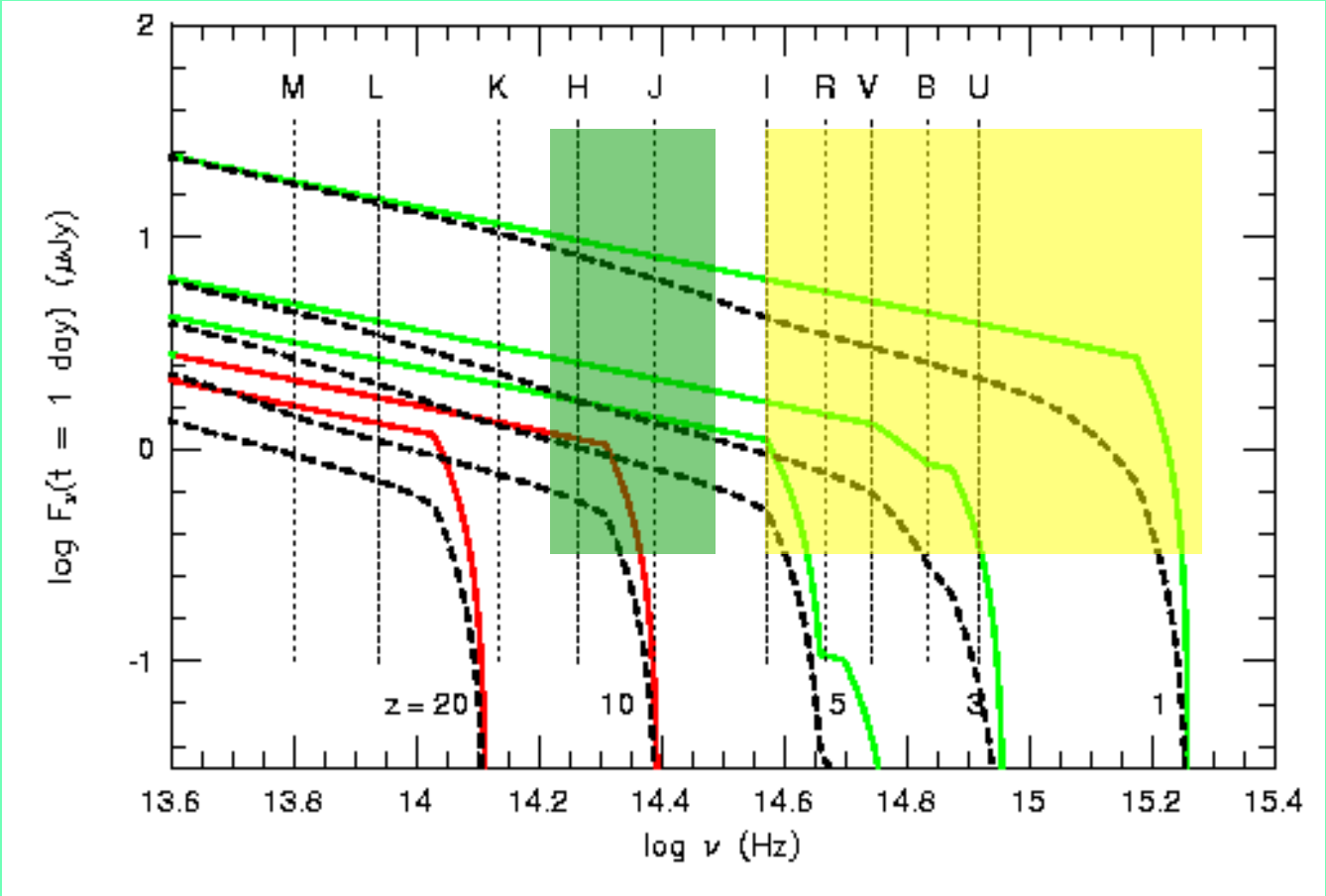

MISTICI (2005)

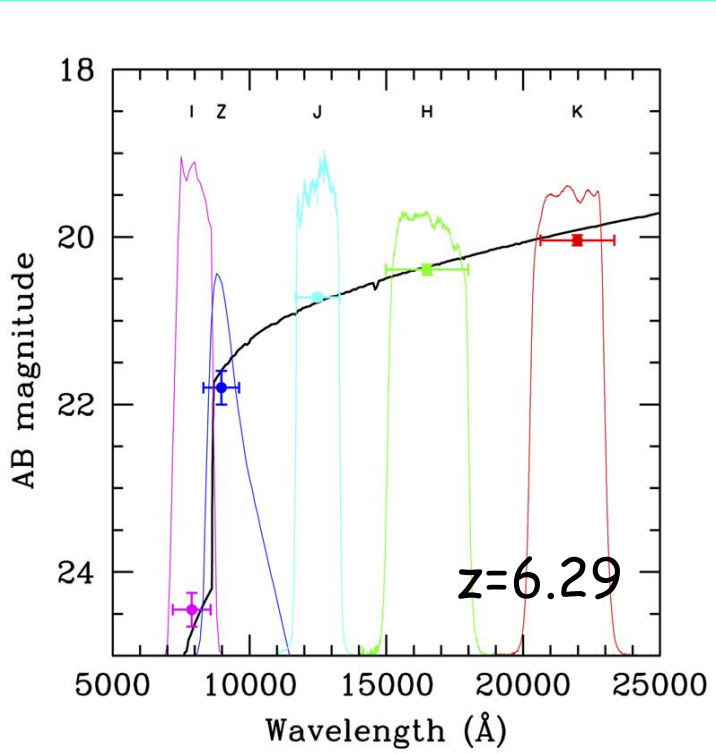

Spectral Energy Distribution of GRB050904

From simplicity to complexity!

From the Dark Ages to the Cosmic Renaissance !

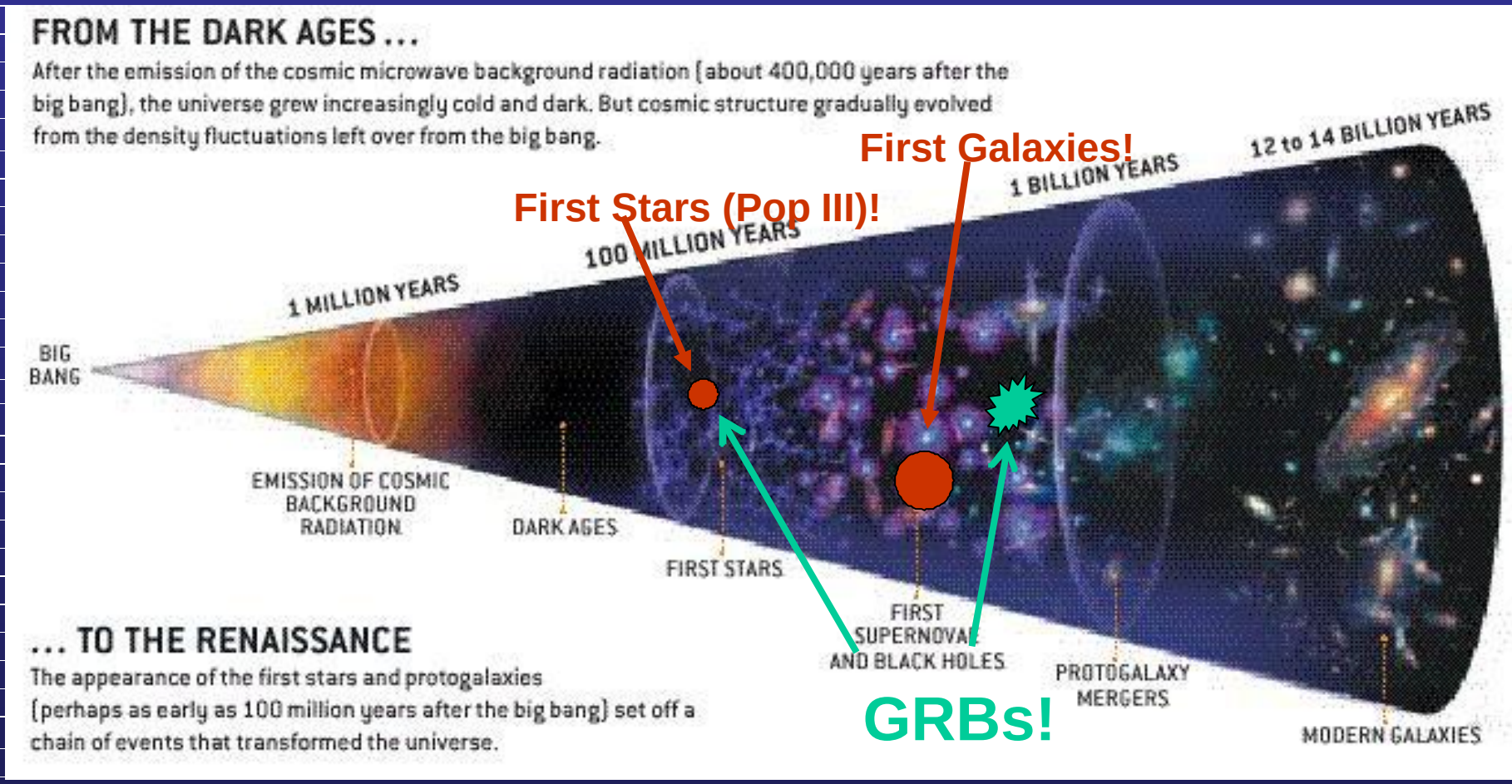

(Larson & Bromm, Scientific American)!

The fraction of high-z GRBs from optically selected samples

- 5.5 +/- 2.8 %
  z > 5 (Greiner+ 10)
- < 14 %, < 7 %
  z > 5, z > 7 (Perley+ 09)
- 3-5 %, 0.2-0.7 %
  z > 5, z > 8 (Salvaterra+ 12)
- < 14 %, < 5 %
  z > 6, z > 7 (Jakobsson+ 12)
- cp. SDSS/CFHT QSO:
  (~0.05 %) z > 5.7 (Willott+ 10)

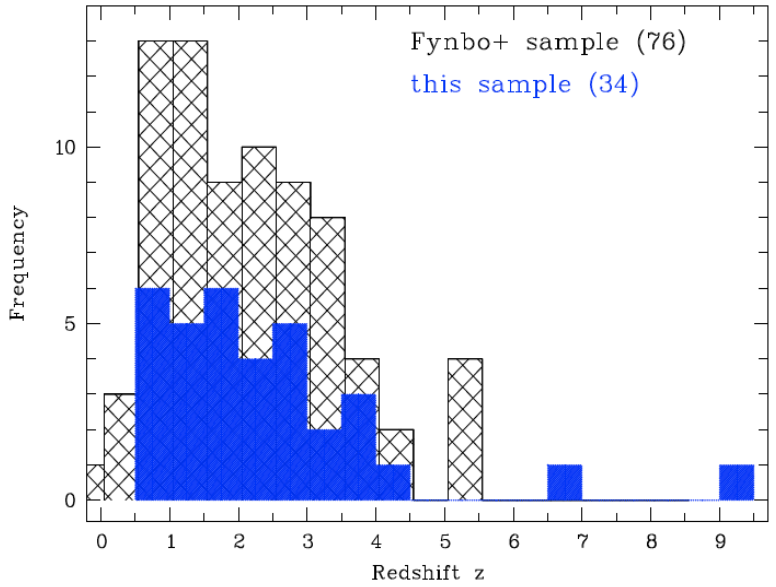

(Greiner+ 10)

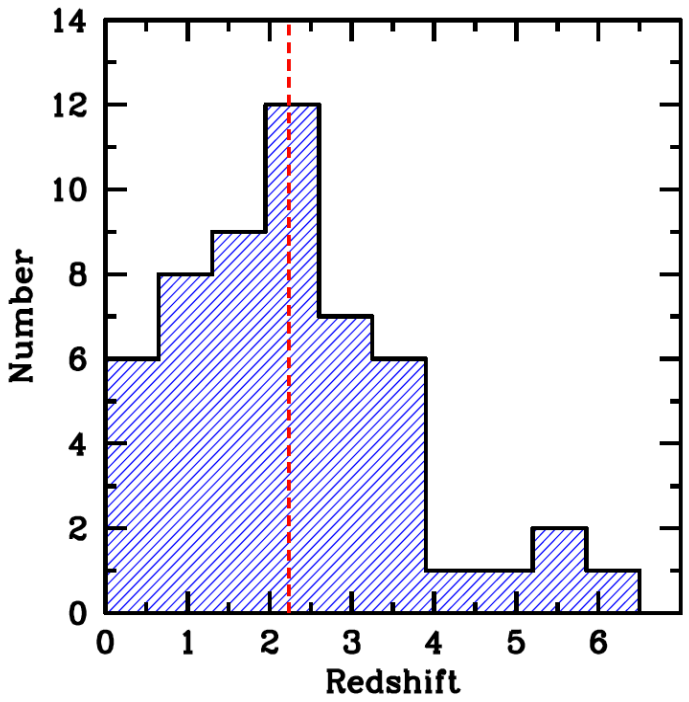

(Hjorth+ 12, Malesani+ 12, Jakobsson+ 12)

Courtesy by T. Kruhler@GRB2012

How many high-redshift GRBs?

Richardson & Ellis 2012

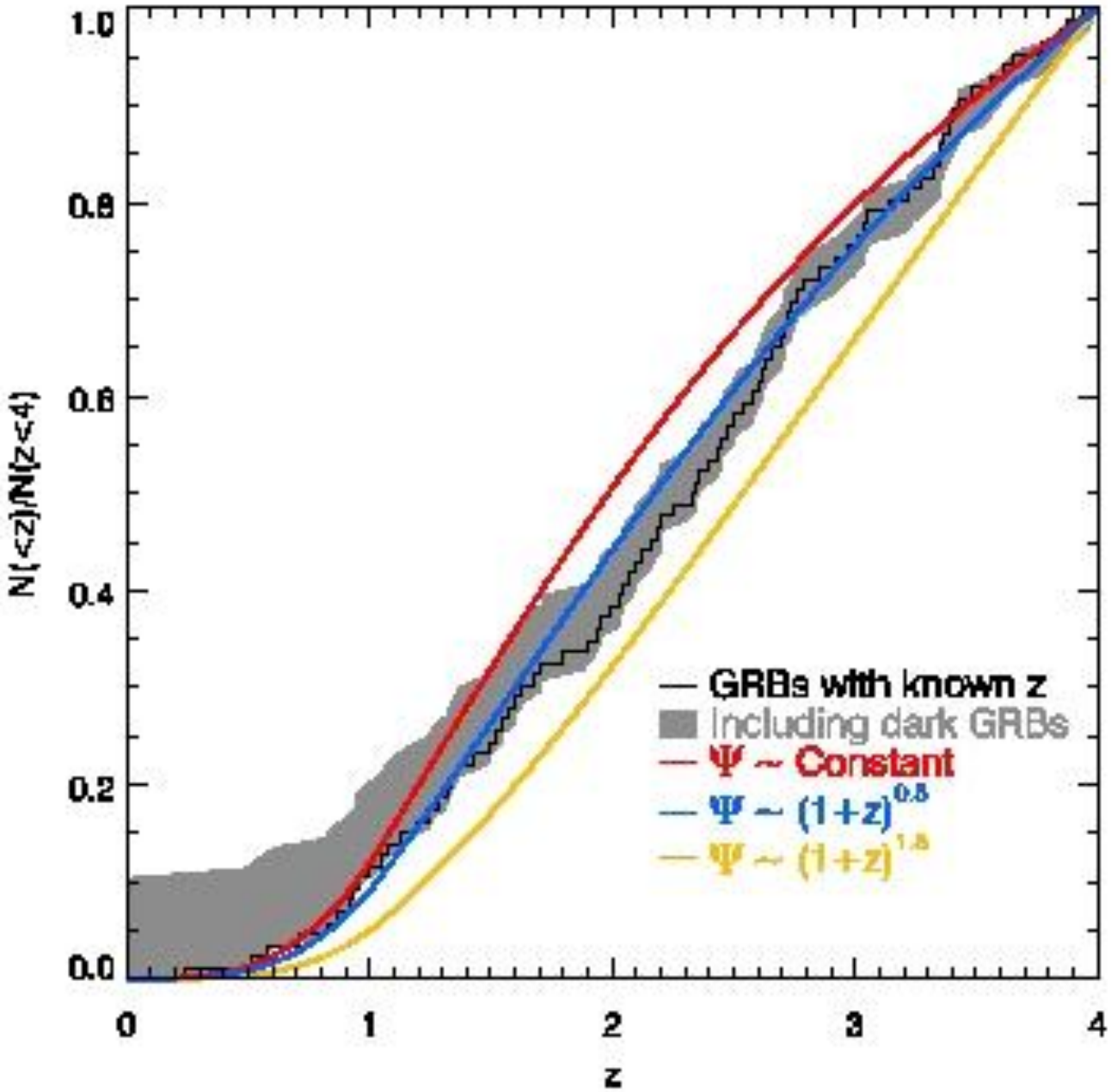

How many high-redshift GRBs?

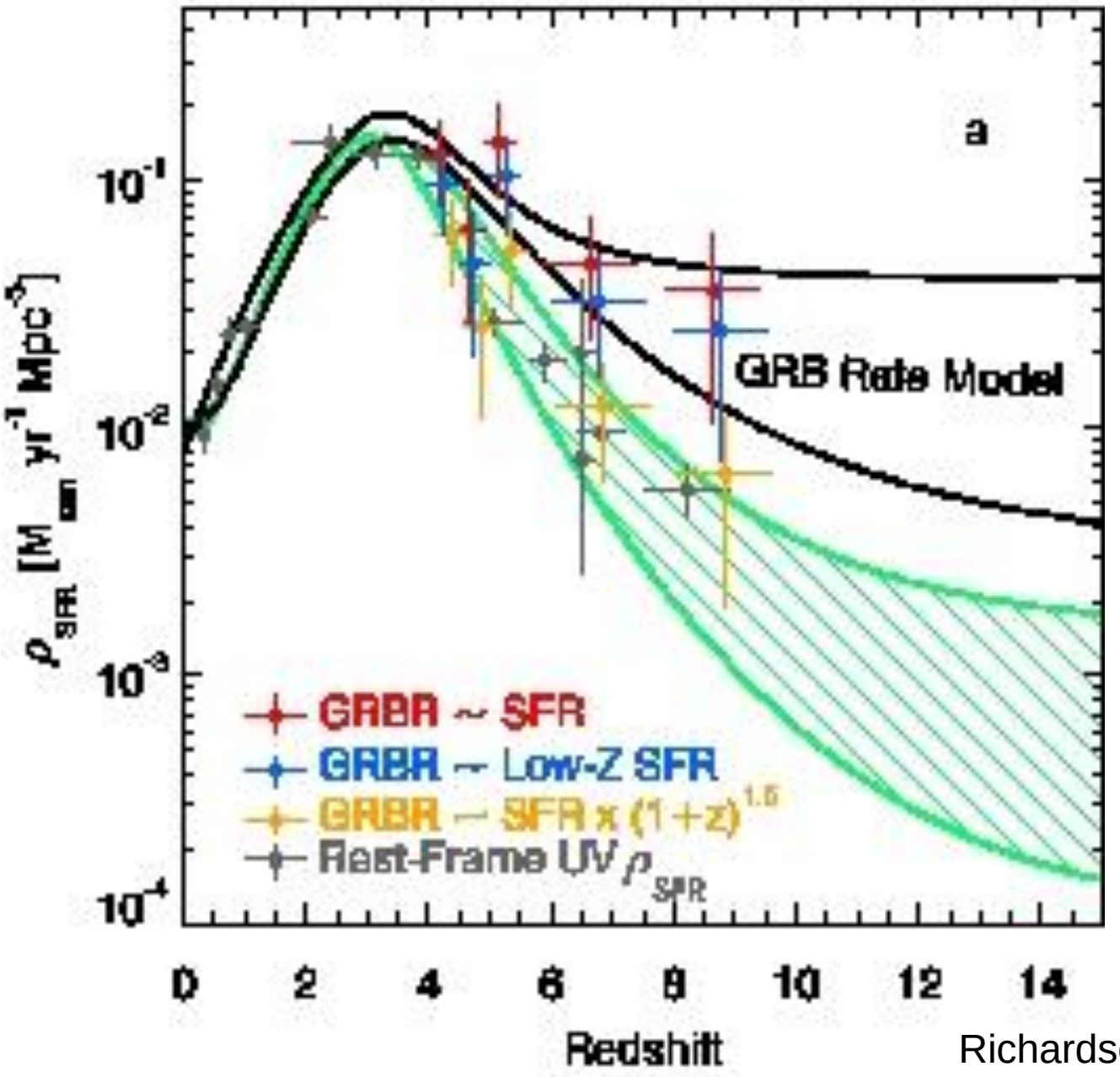

Richardson & Ellis 2012

Based on the highly complete GROND LDGRB sample, Elliott, Greiner, Khochfar et al. (2012) conclude that the LDGRB rate is proportional to the SFR independently of the metallicity and/or of the host galaxy type!!!, i.e., $\acute{\eta}_{LDGRB} \sim \acute{\eta}_{SFR}(1+z)^{\delta}$, with $\delta = 0$

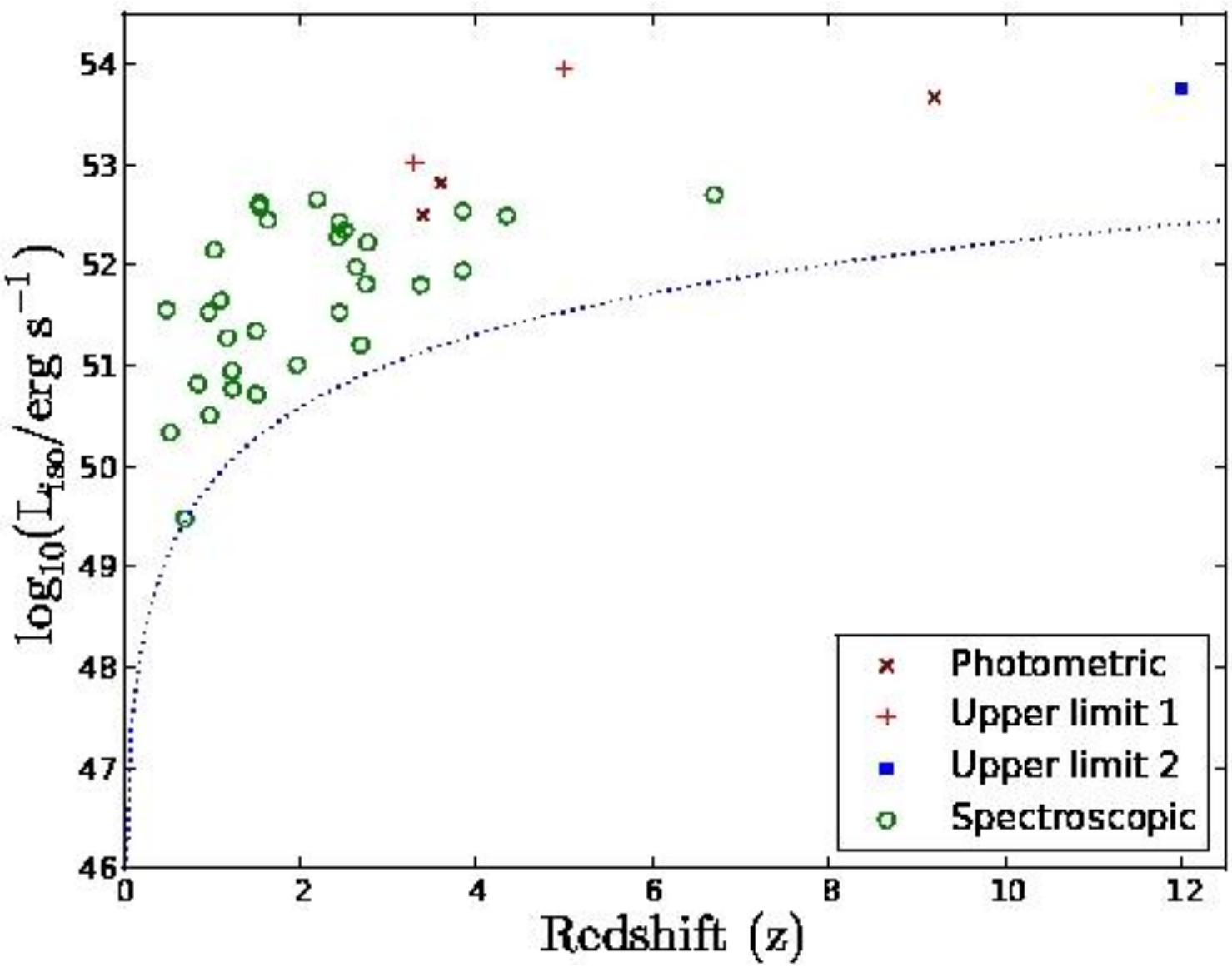

Elliott+ 2012

Expected rate of GRBs from PopIII.1 stars, formed with M_{init}~1000 $M_{\odot}$

De Souza,Yoshida and Ioka (2011)

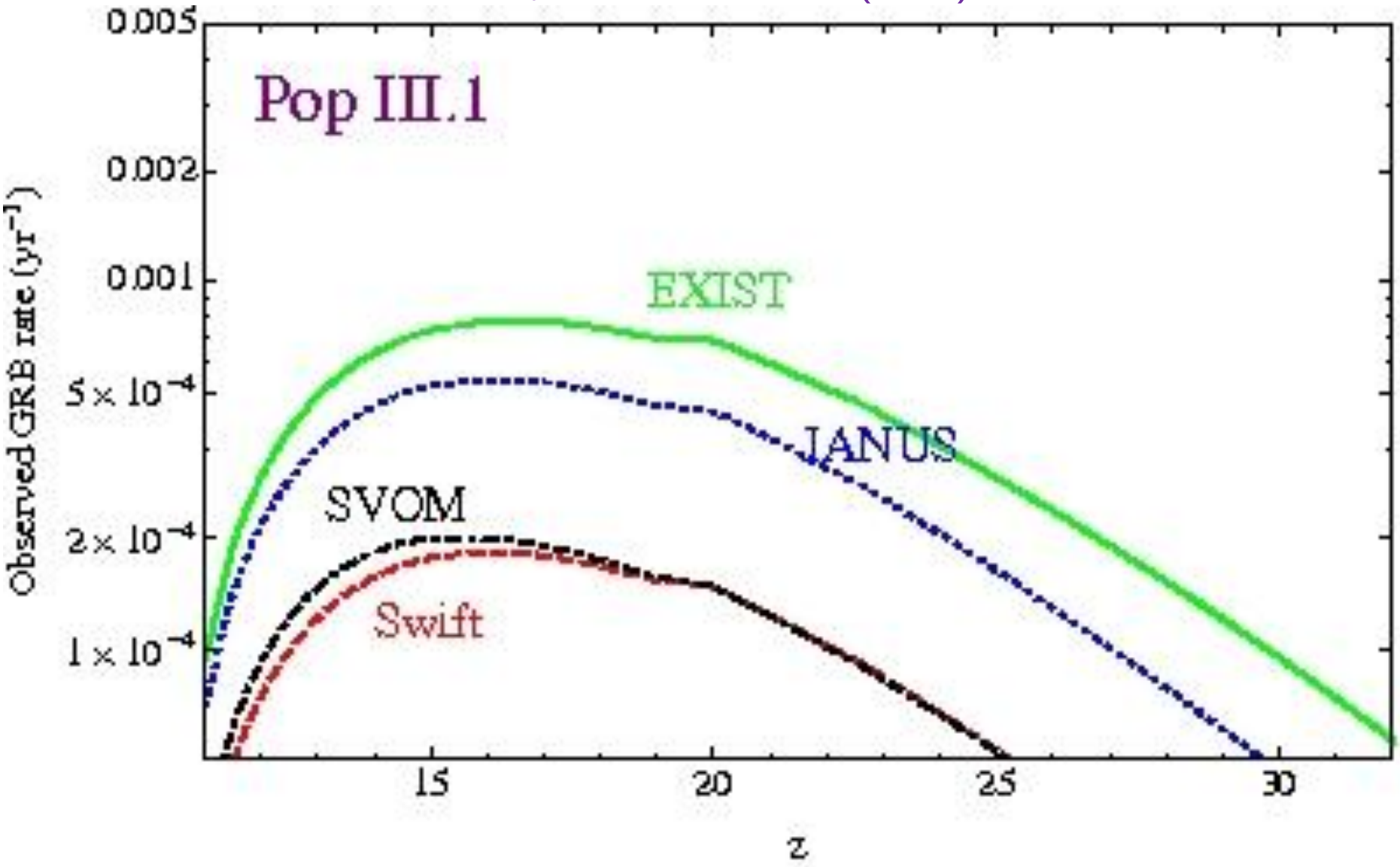

Expected rate of GRBs from PopIII.2 stars, formed with M_{init}~40 - 60 $M_{\odot}$

De Souza,Yoshida and Ioka (2011)

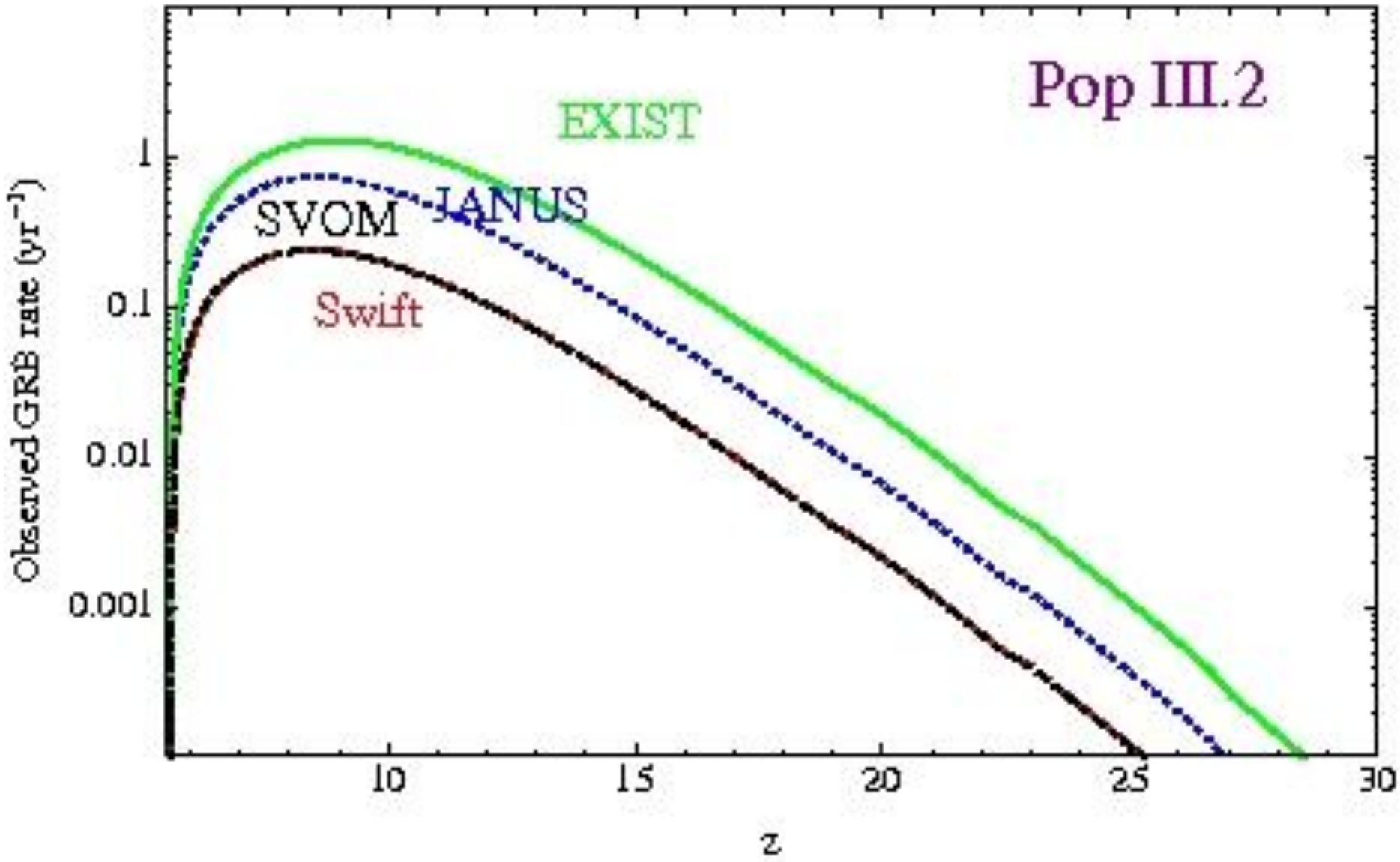

Simulation results of the first generation stars formation.

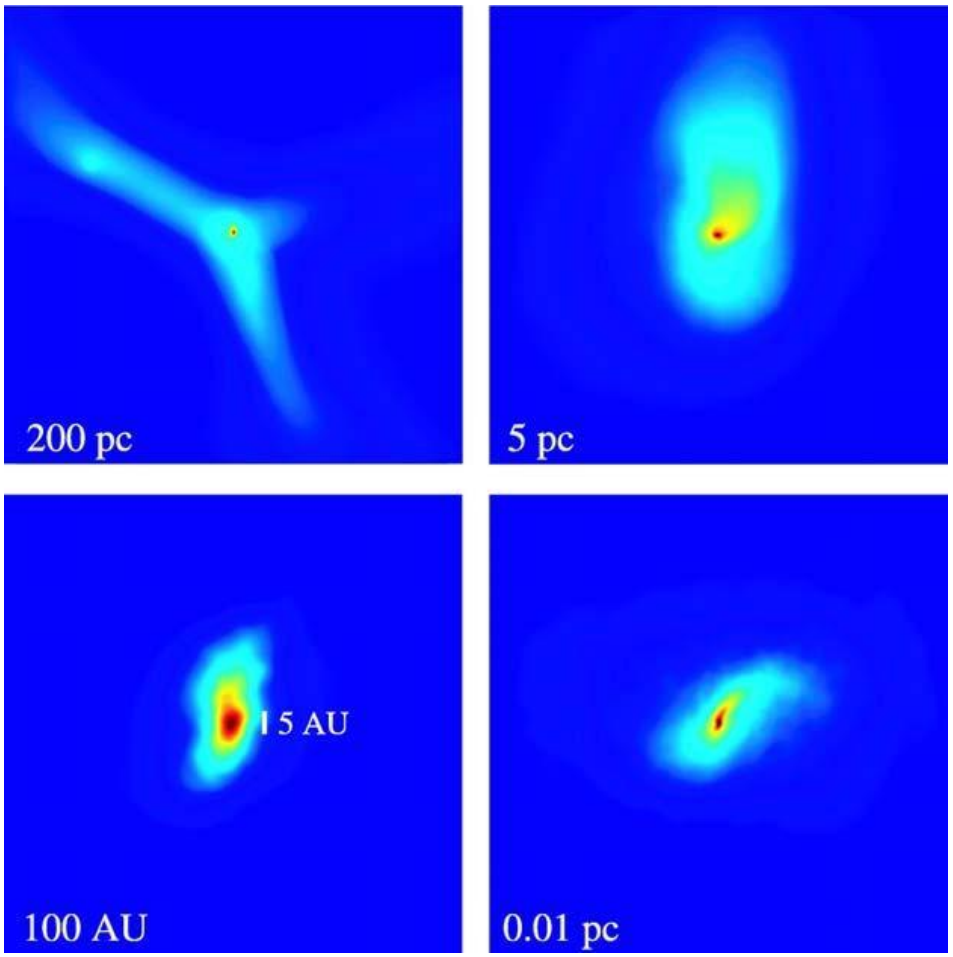

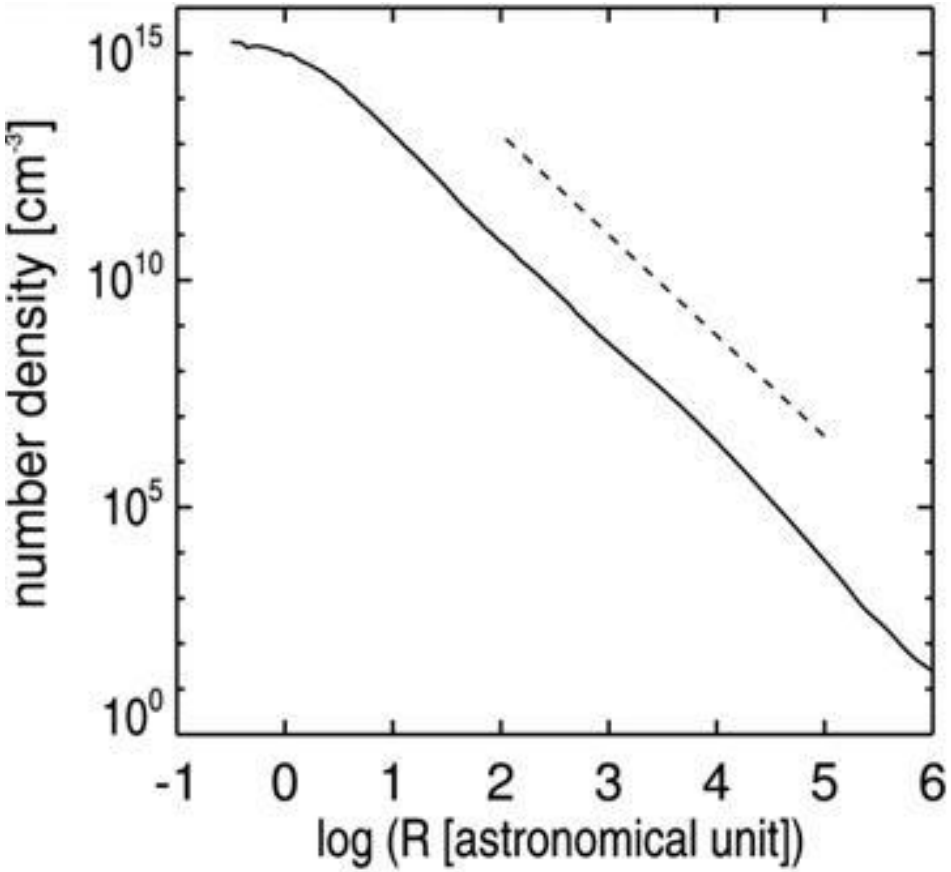

Density profile of the first generation stars from Yoshida et al. (2006). Note, that each dex in Log(R), contains ~10^{28} cm^{-2} of the hydrogen column.

Resonance γ-photon absorption

(Iyudin et al 2005)

- PDR – Pygmy resonance: produced by the resonance capture of photons on levels with energies of ~ 7 MeV

(Axel 1962; Hayward 1977; Van Isacker et al. 1992)

- GDR – Giant Dipole Resonance: process that is crudely described as oscillation of neutron fluid relative to protons

(Goldhaber and Teller 1948; Migdal 1949; Ahrens 1985; Eramzyan et al. 1986)

- Delta-resonance – absorption of photons with an energy ~325 MeV by a nuclei via formation of the Δ-isobar, that leaves a target nuclei and π-meson(s) in the exit channel

(Ahrens 1985; Hagiwara et al. 2002)

HI →n<10^3 cm^{-3}; H_2O masers →n_{cr}>10^{10} cm^{-3}; CS(J=7→6) →n_{cr}>2.8x10^7 cm^{-3}

$N_H$columns

CS(J=5→4) →n_{cr}>8.9x106 cm-3, HCN →n_{cr}>3x104 cm-3, CO →n_{cr}>500 cm-3

Zwaan et al. (2005); Larson (1981), McKee (1999) → N_H~(1.5 0.3)x10^{22}xR(pc)0 0.1 cm^{-2} ; but Shirley et al. (2003) claims N_H from CS measurements that are a factor of ~20-50 higher; examples S106, NGC7538

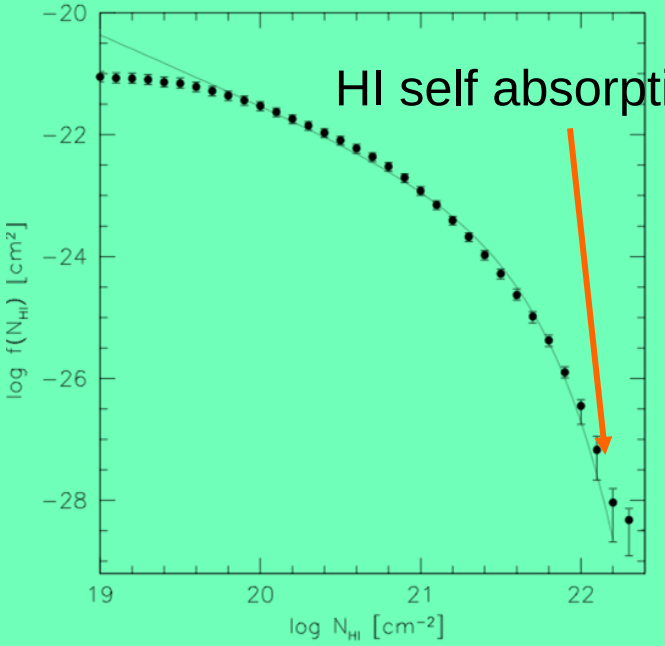

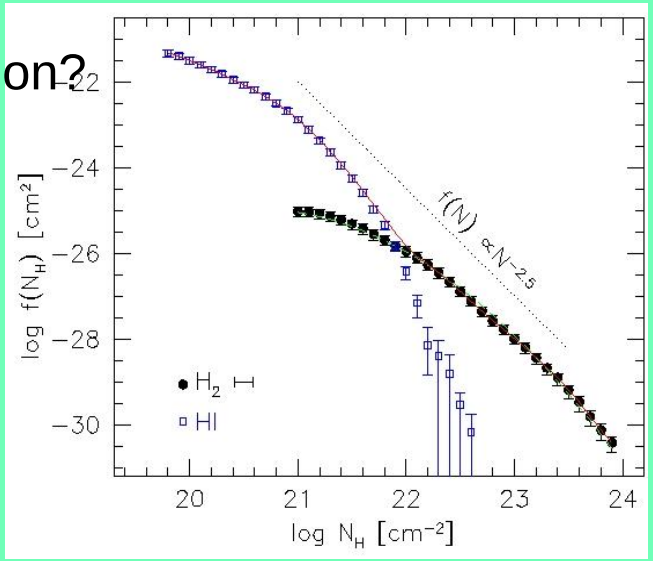

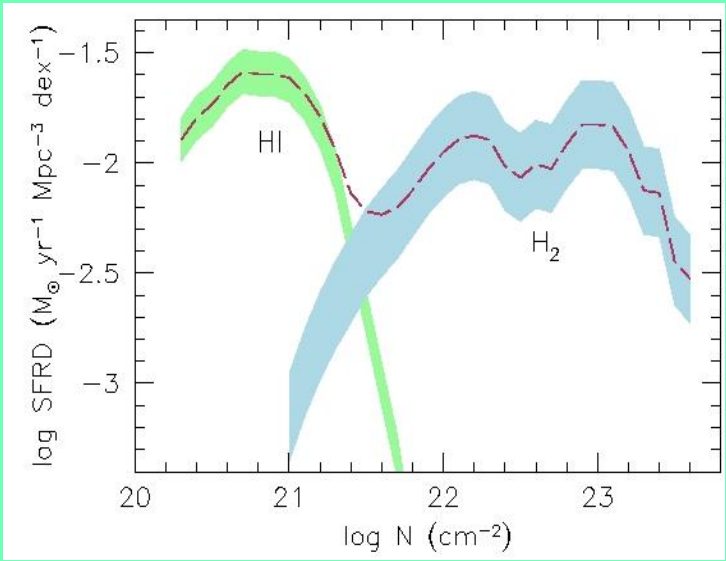

Generally, N_H measured at different λ are different-Arav et al. (200

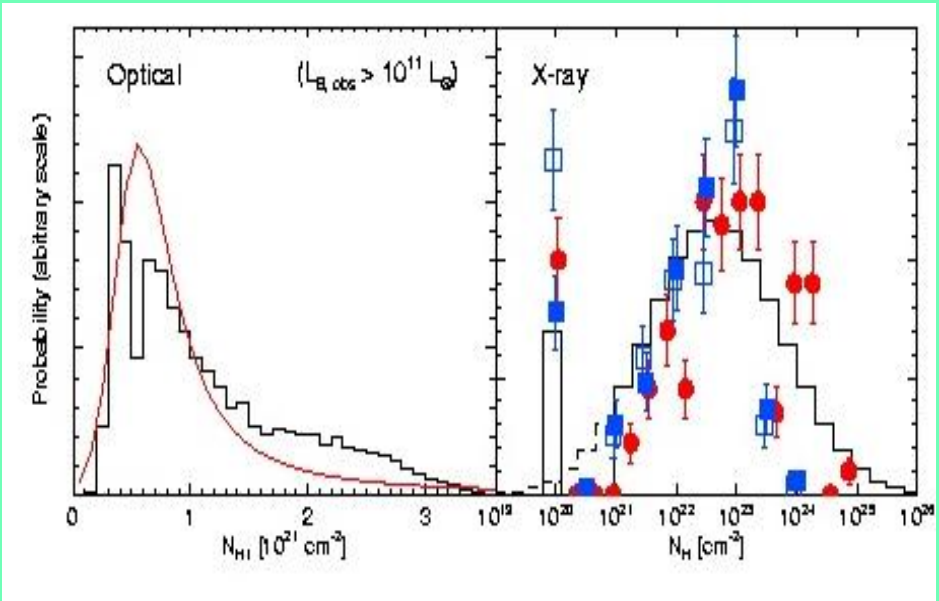

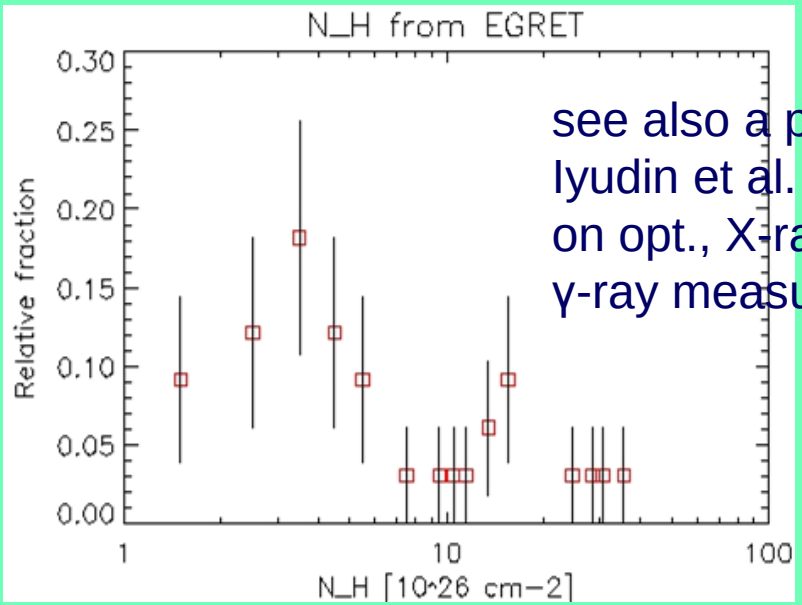

see also a paper by Iyudin et al. (2005) on opt., X-ray and γ-ray measured N_H

N_H from optically selected GRB samples

Courtesy by T. Kruhler@GRB2012

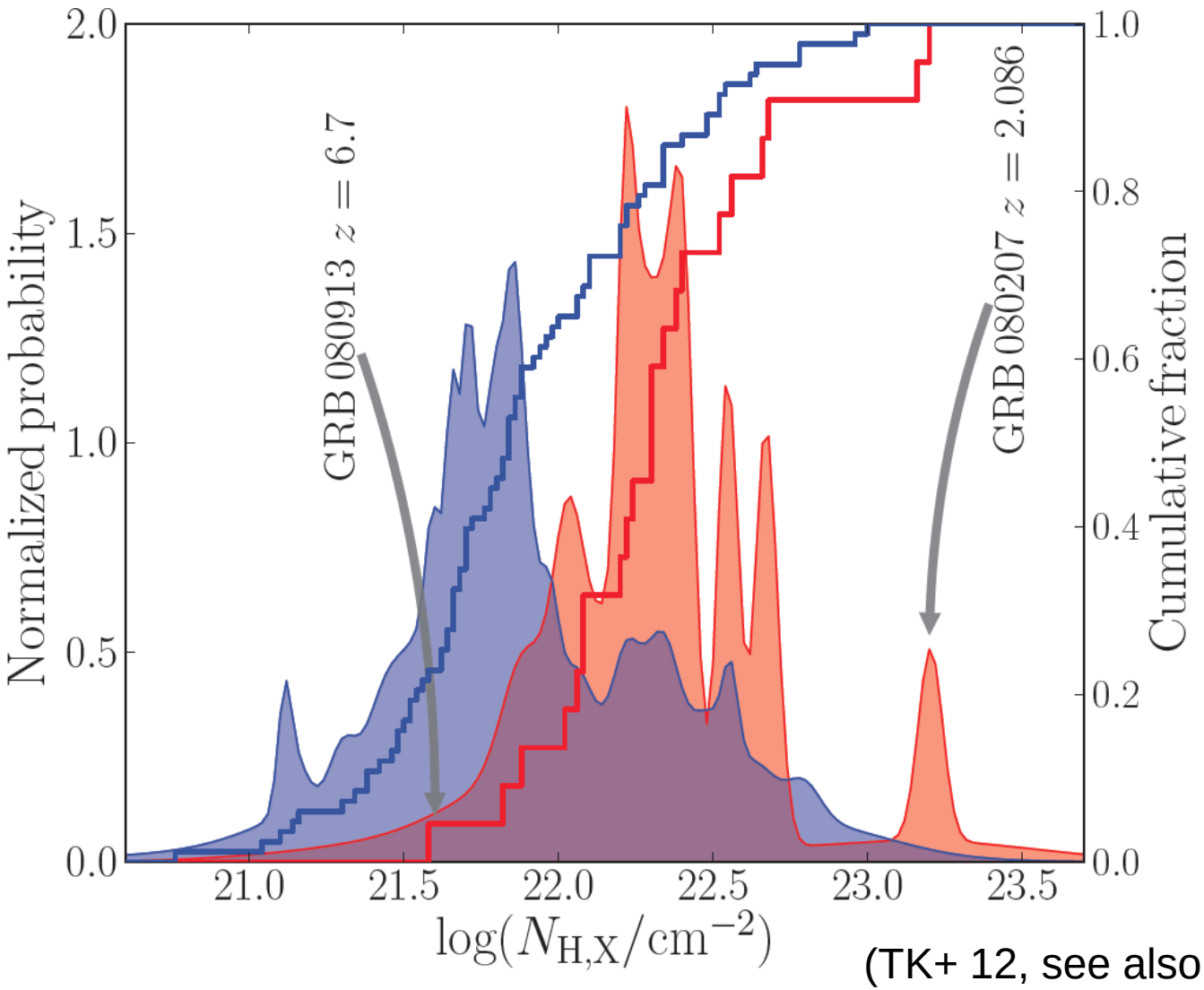

Redshift dependence

- Little redshift information in low-res X-ray spectra
- Get redshifts from optical
- But! Inferred absorption strongly redshift dependent:
- $N_{\mathrm{H_X}}(z) \approx (1+z)^{2.5}\, N_{\mathrm{H_X}}(0)$

This problem is amended by NRA application!!!

(TK+ 12, see also Fynbo+09, Campana+12)

Cross section of γ-photon absorption on the nuclei of ^{1}H as measured by MacCormic et al. (1996.

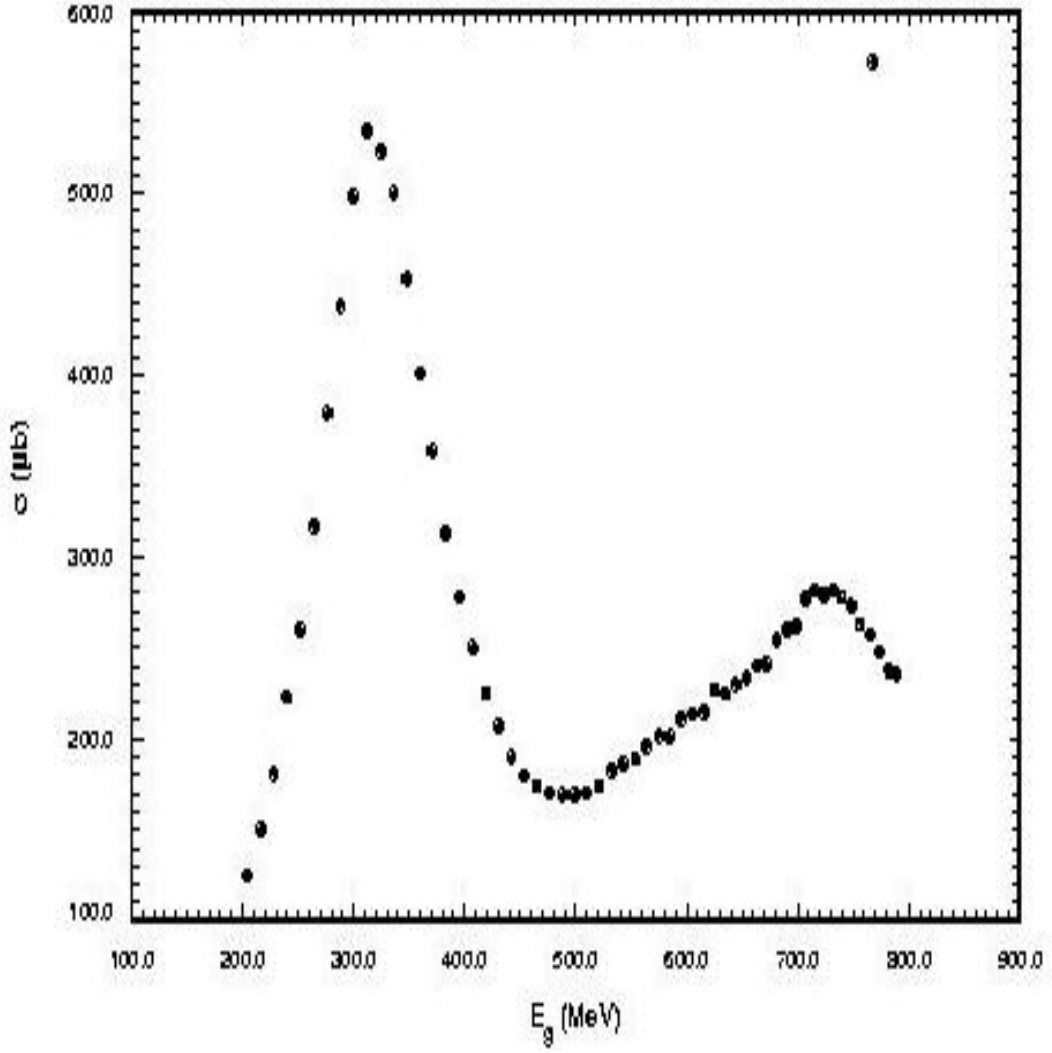

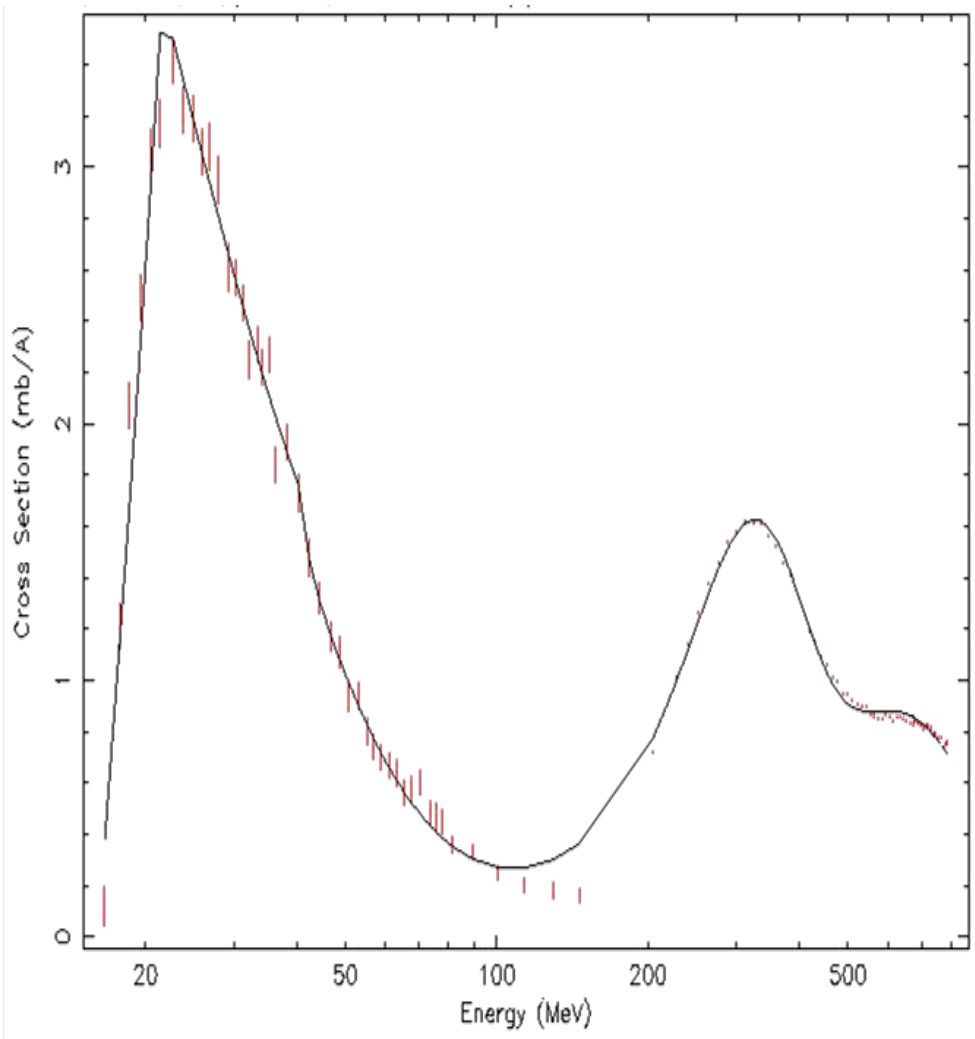

Cross section of γ-photon absorption on the nuclei of ^{4}He (MacCormic et al. 1997).

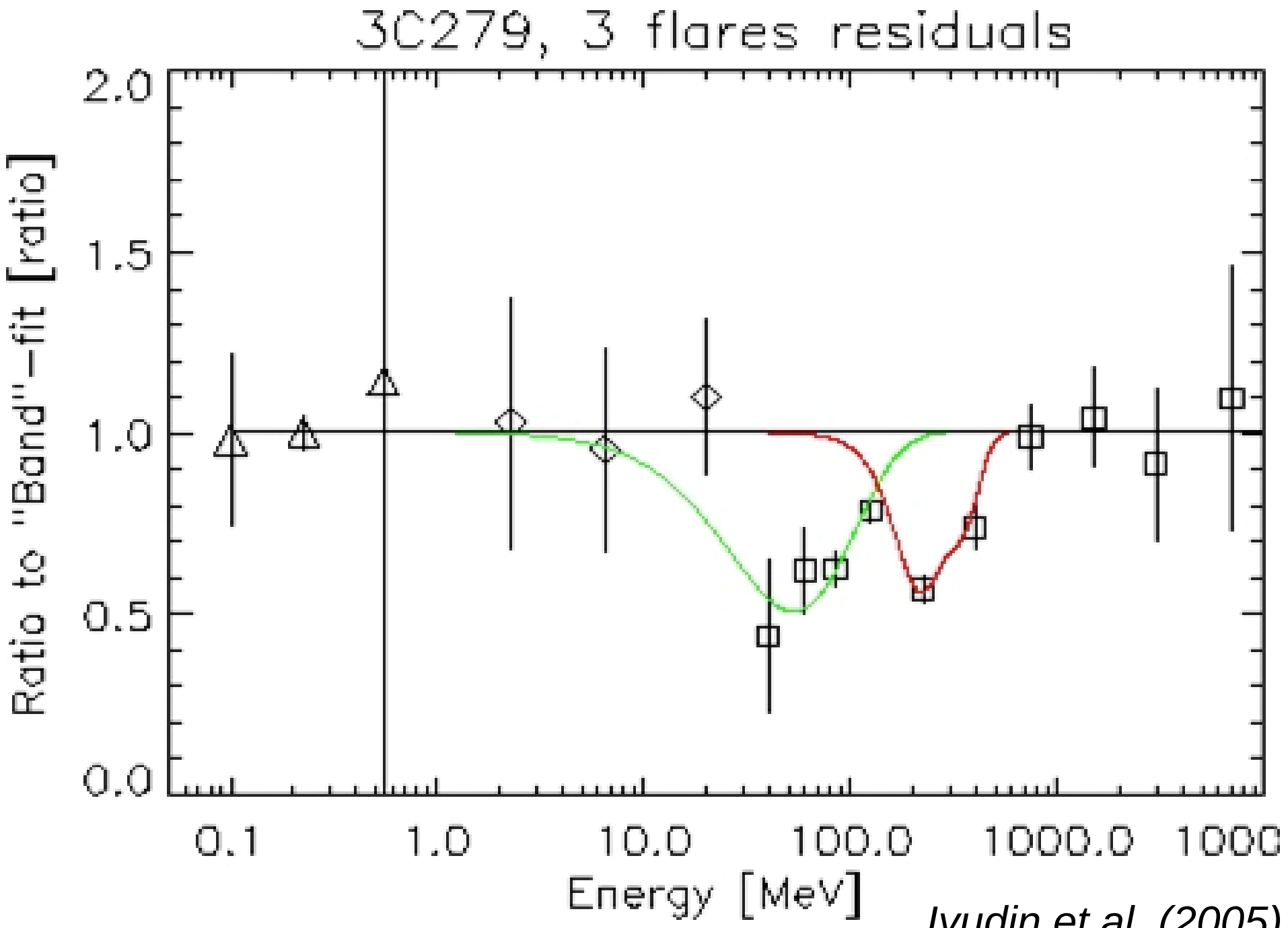

Iyudin et al. (2005)

Energy range selection for the GRB monitor

To cover energy range of resonance absorption troughs for high-redshift objects, GRBs and QSO, gamma-ray monitor has to have a spectral capability for γ–rays in energy range from ~1 MeV to 70 MeV (see also Iyudin+05;07; Greiner+09)

In order to exploit polarization measure as an instrument to distinguish an emission mechanism in central engines of GRB or QSO (blazar) gamma-ray monitor has to have an energy range for γ–rays detection from ~10 keV to 1 MeV

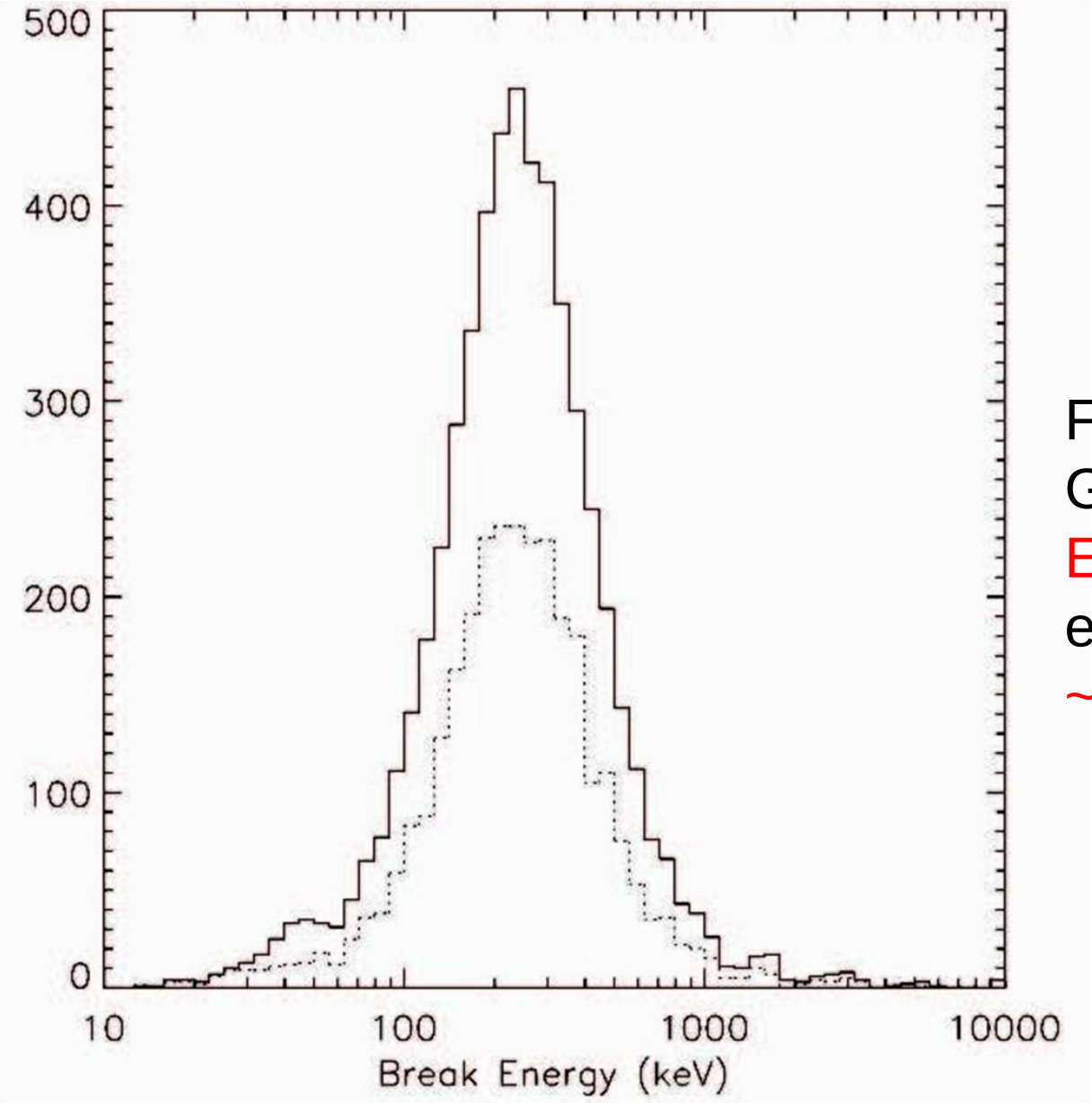

For high redshift (z>10) GRBs the peak energy E_p distribution will cover energies typically from ~1 keV to ~200 keV !!!

Distribution of the GRB peak-energies for BATSE detected bursts (adopted from a paper by Preece et al. 2000).

Proposed energy ranges for the GRIPS experiment monitors

Greiner et al. (2011)

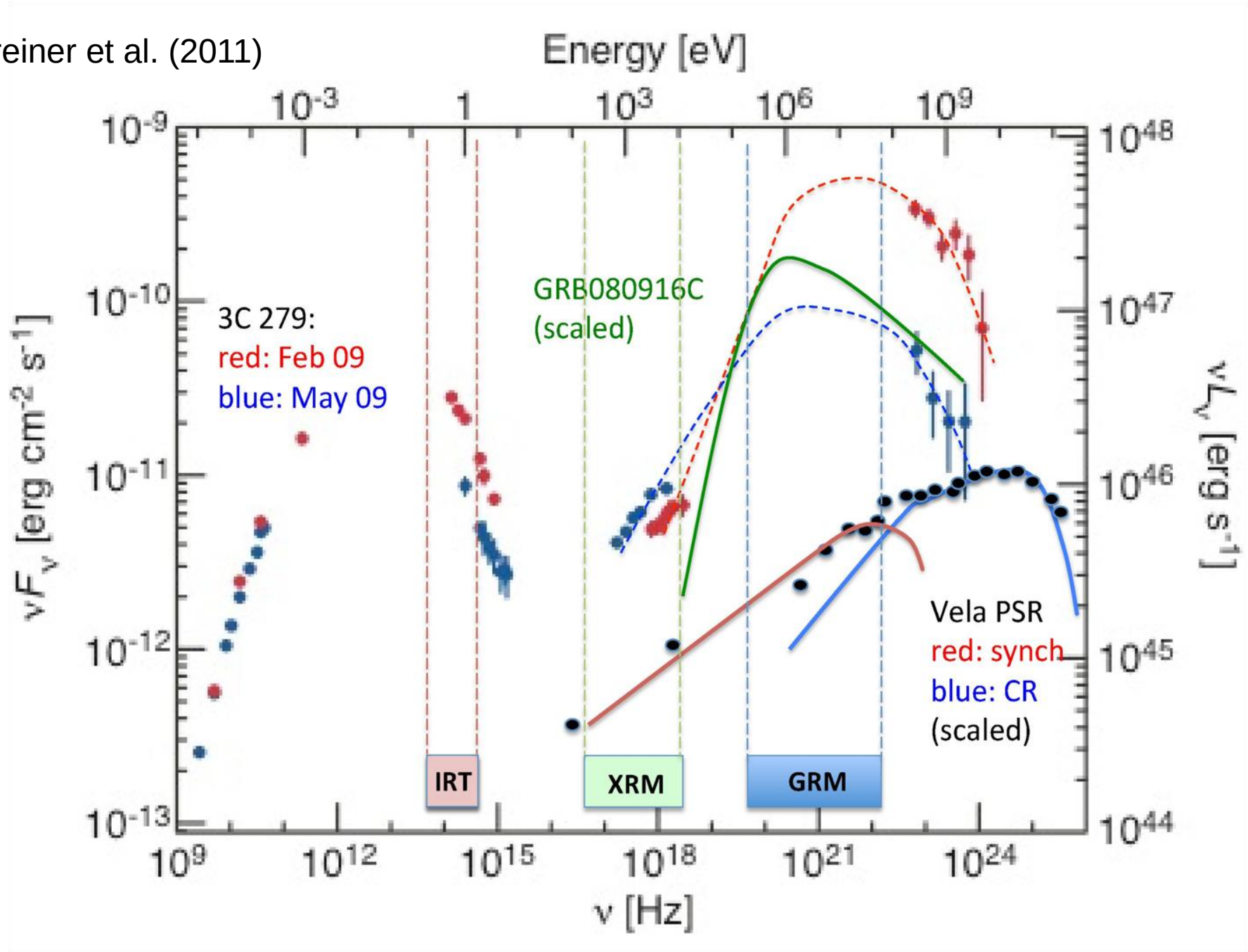

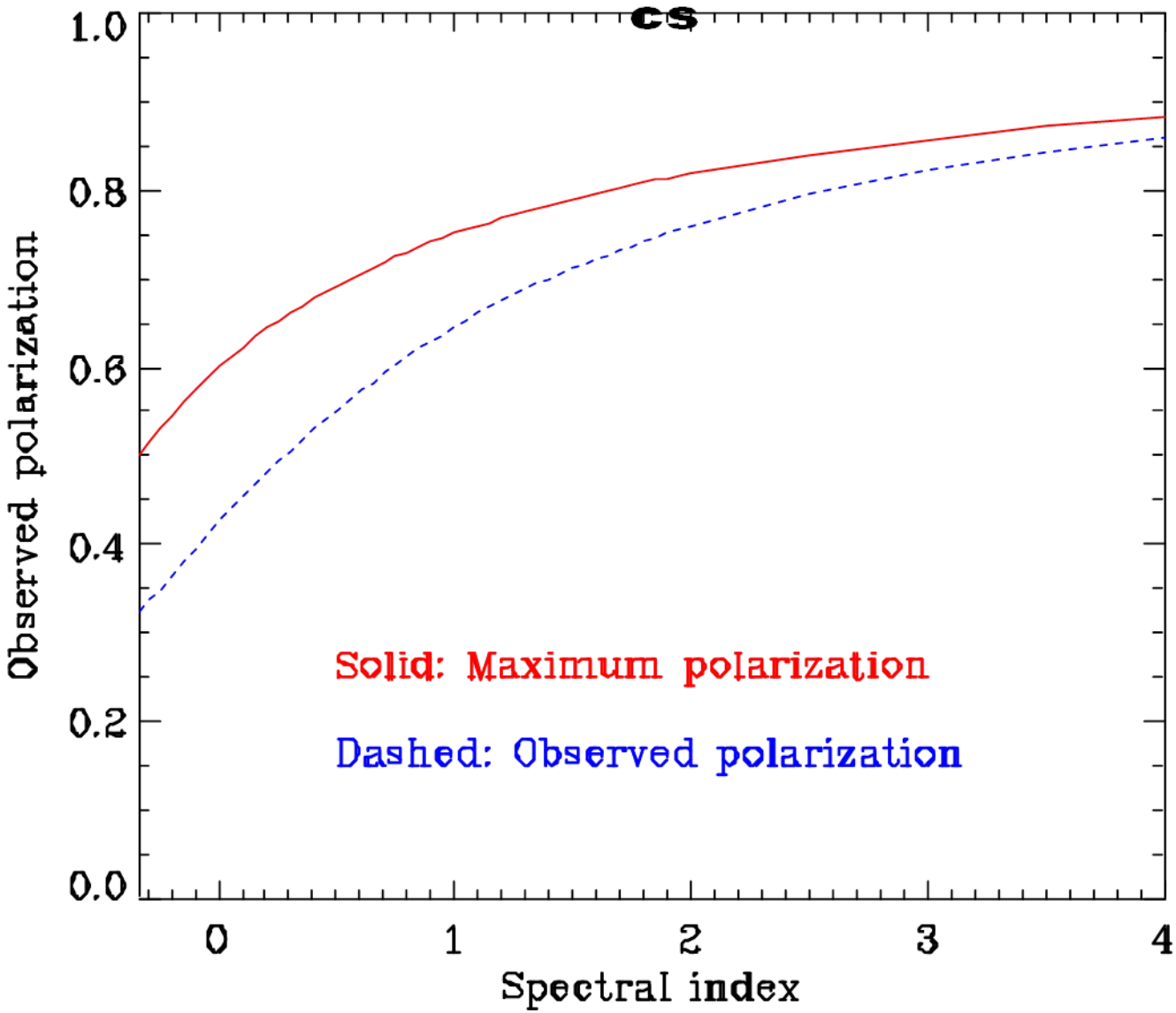

Lazzati (2006)

Figure 7. Resulting polarization of the prompt emission of GRBs from a completely aligned magnetic field as a function of the power-law spectral index. The red line shows the theoretical maximum polarization while the blue dashed line shows the polarization that is observed after light aberration has been taken into account. The result is relevant for the time integrated emission.

Conclusions I

- Open questions:

  -> Role of magnetic fields (Reverse shock, polarimetry …) (-> Talk by Ph. Laurent)

  -> Long-term activity of the central engine

  -> Temporal evolution of the microphysical parameters

Conclusions II

- GRB cosmology holds tremendous promise!
- GRBs are ideal signposts of the first stars and galaxies
- GRBs are expected to have the highest high-z rate (~5% @ z > 5, factor of 100 higher than that of QSOs)
- GRBs are ideal probes of early IGM metallicity, dust and of host galaxy properties
- Missions capable of detecting high-z GRBs are vitally important to advance GRB cosmology of the early Universe to the maturity!!!

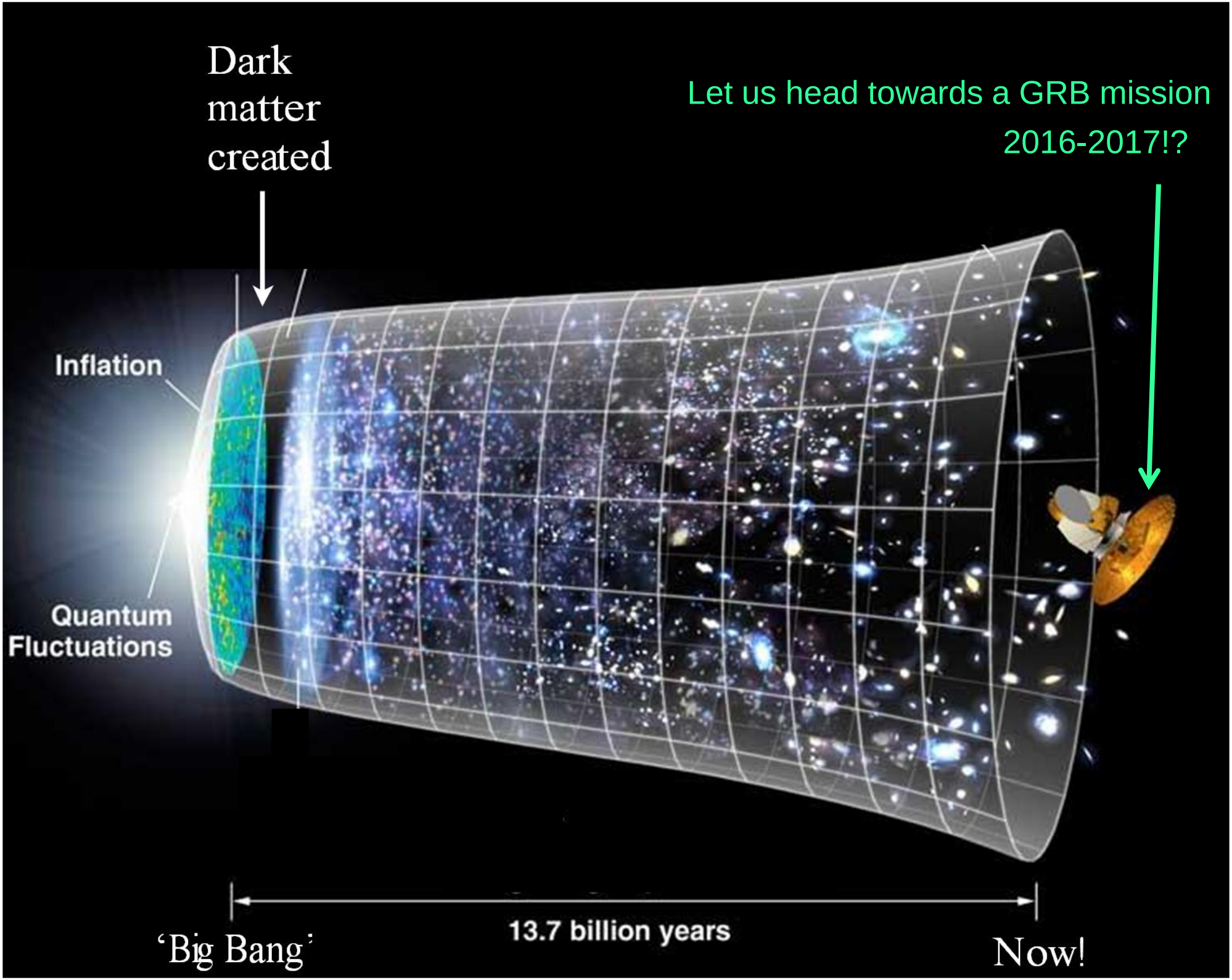
Dark matter created
Let us head towards a GRB mission 2016-2017!?
Inflation
Quantum Fluctuations
13.7 billion years
'Big Bang'
Now!

Detection of γ-quanta

Classical Compton Event Circles (no electron tracking)

Reduced Compton circles of events with electron track

Direct imaging of pair-creation events

← 2 MeV →

← 8 MeV →

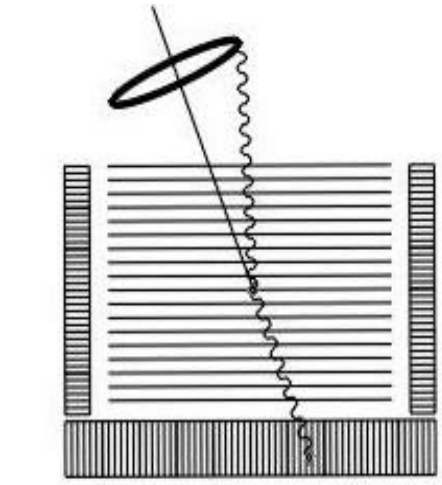

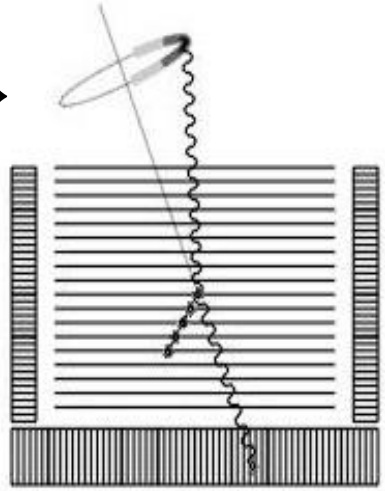

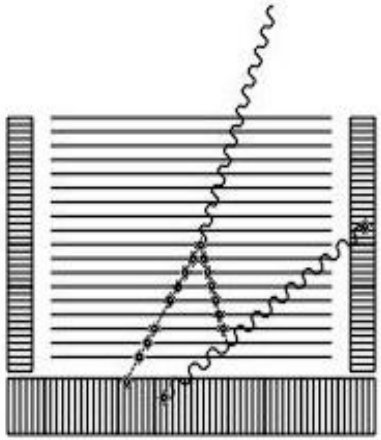

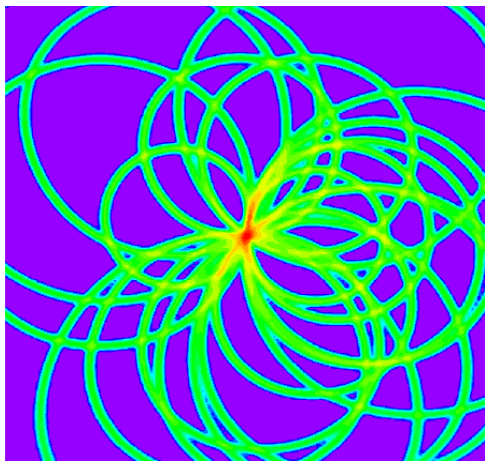

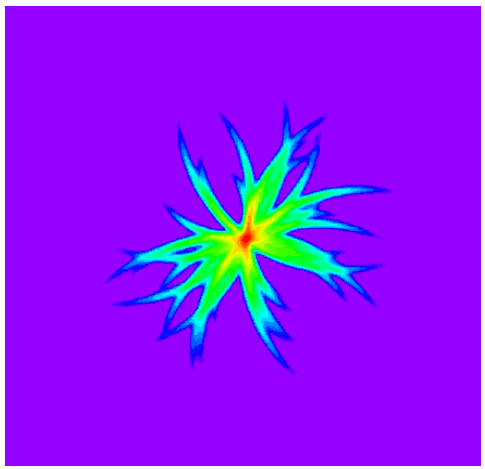

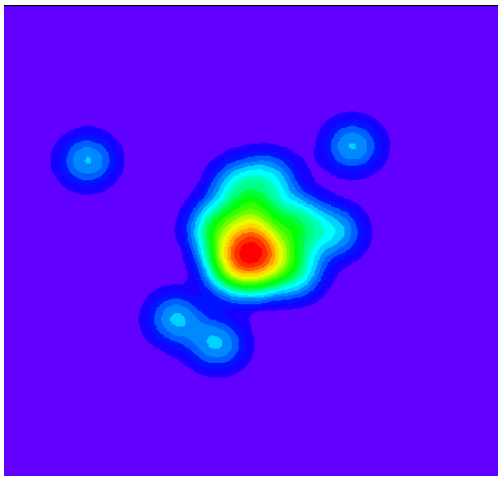

“GROME-S” – Wide Field-of-View Gamma-Ray Monitor.

GROME-S is a scaled down version of GROME-GRIPS (Greiner et al. 2009),
that will be factor of 4 smaller than GRIPS in effective area,
but still will have ~10 better sensitivity than COMPTEL.

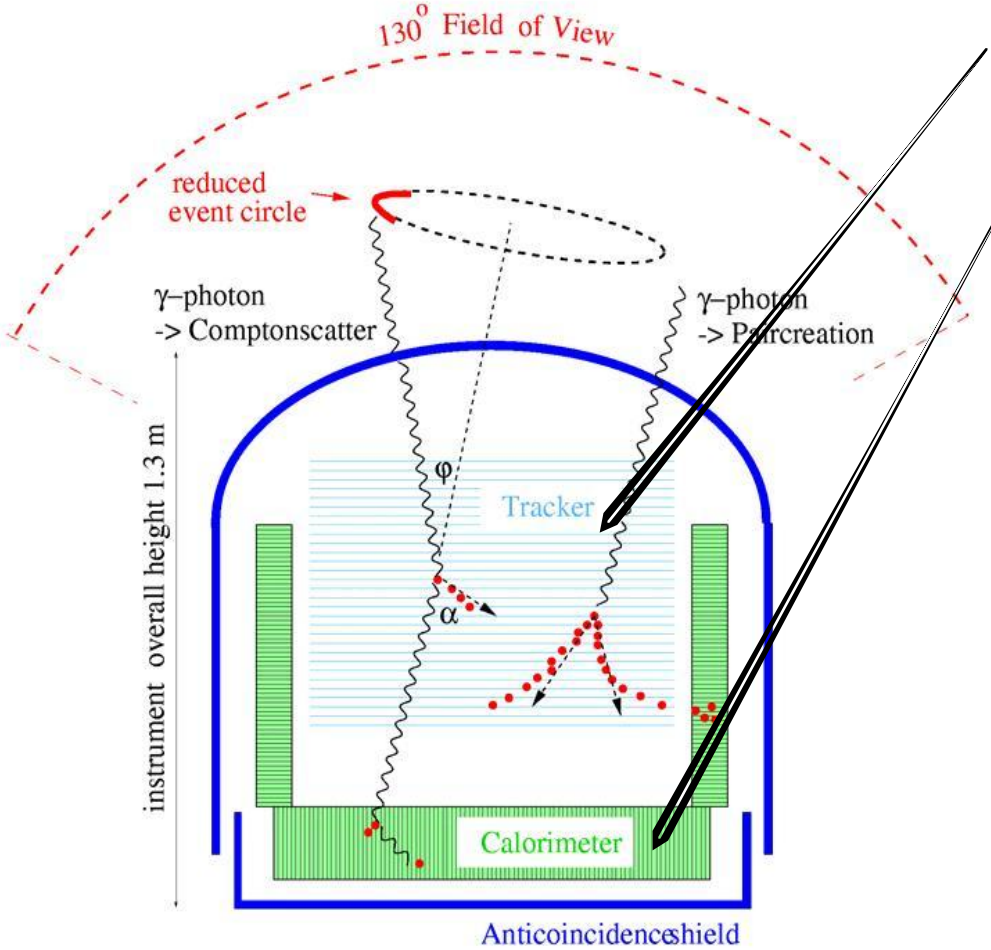

Tracker: double sided Si strip detectors

Calorimeter: 3D resolving $LaBr_3$ / Si drift diode

Images

Classical Compton | Tracked Compton | Pairs

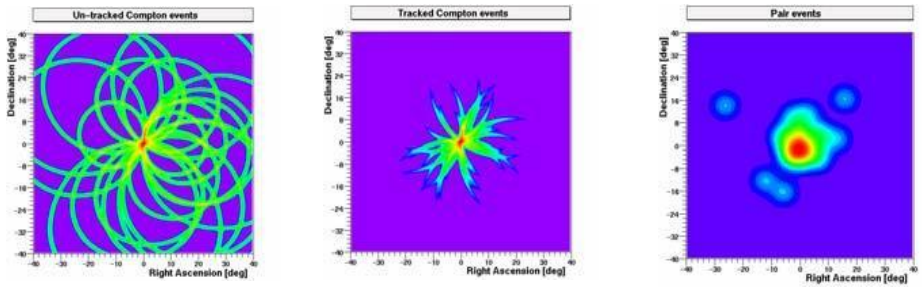

Principles of MeV-photons detection by GROME-S (left), and results of image reconstruction for a point source with Compton telescope detected photons, that can operate also in a regime of detecting e-,e+ pairs produced in a pair-conversion process at higher gamma-energies (>10 MeV) (right) (adopted from a paper by Kanbach et al. 2005).

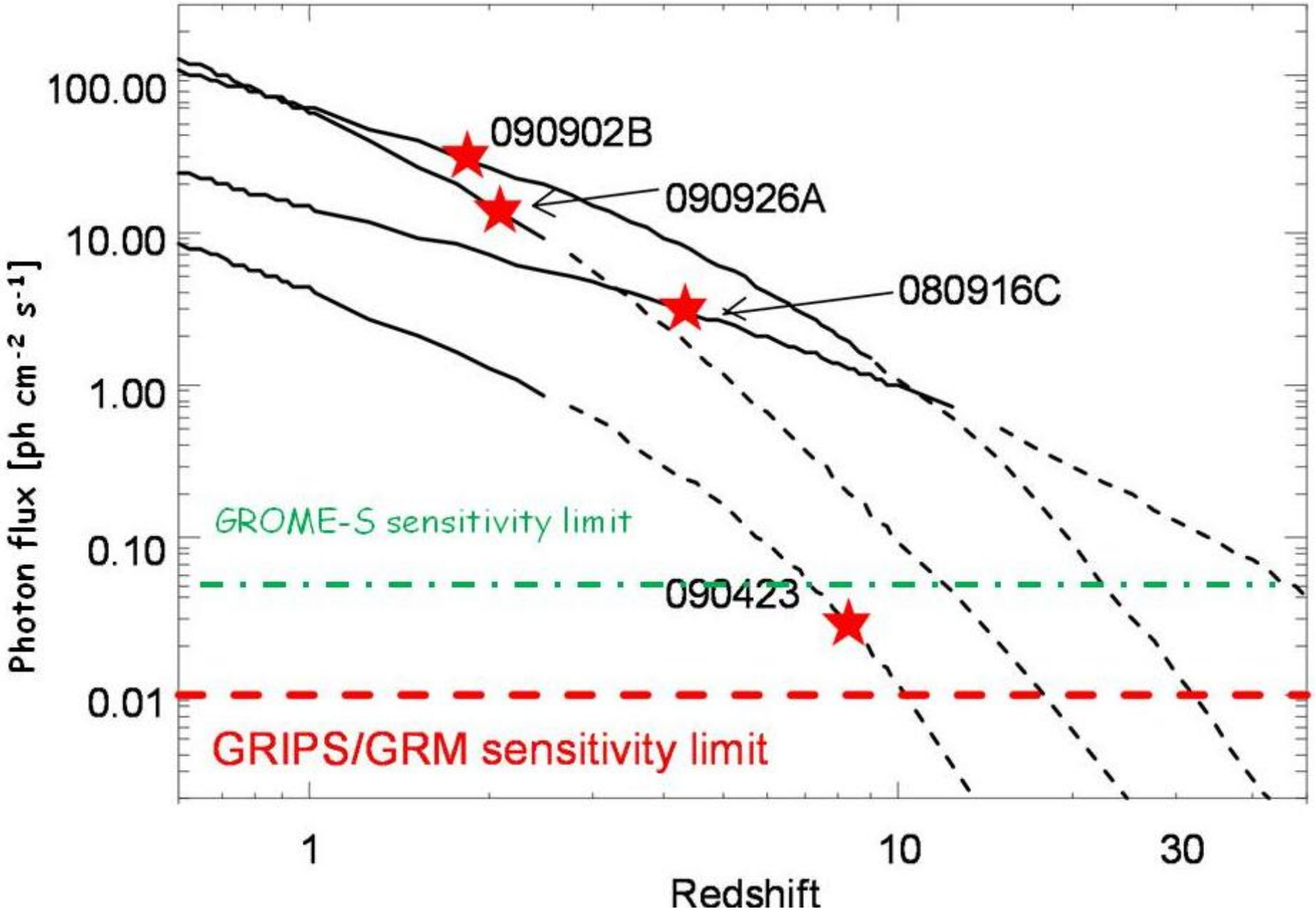

Sensitivity limit of GROME-S scaled down from the one calculated for GROME-GRIPS/GRM. Red stars mark "typical" GRBs at high redshifts, that were detected until present.

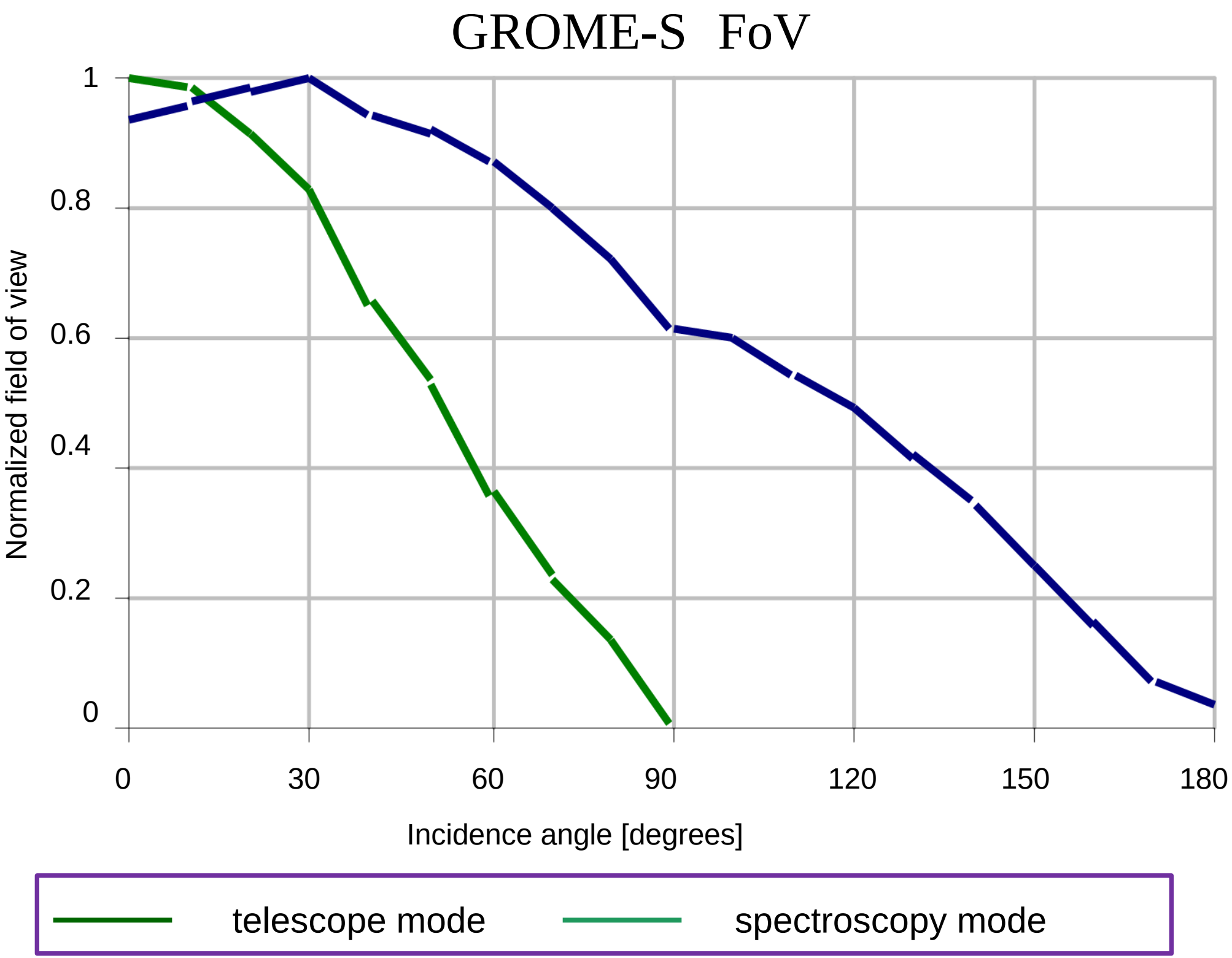
GROME-S FoV
1
0.8
0.6
0.4
0.2
0
Normalized field of view
0
30
60
90
120
150
180
Incidence angle [degrees]
telescope mode
spectroscopy mode

GROME-S would detect ~ 160 GRBs/year;

for a 2 years long mission, ~ 300 GRBs!
Among those we expect to detect:

from >~2 to 20 GRBs at z>10;

and up to 6 GRBs at z>20 !

Response of 20x20x10.5 mm^3 CdZnTe monolithic pixellated detector

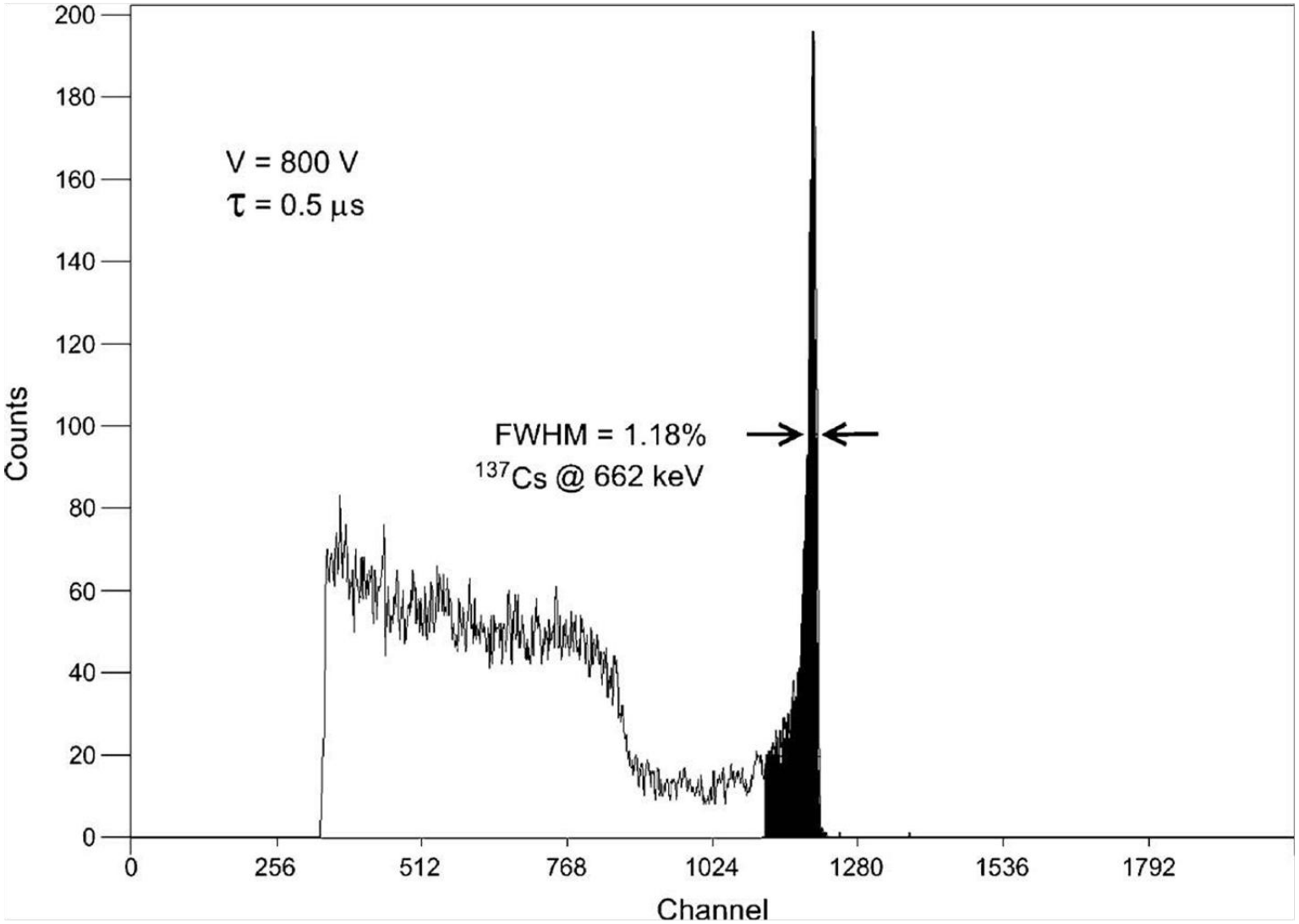

FIG. 8. ^{137}Cs response, 1.18% FWHM, of a single pixel from 20 x 20 x 10.5 mm^3 monolithic pixellated detector pixel size=2.46 mm without any additional signal correction.

P. Chen, S. Ahmad, K. Ahn, et al., 32nd ICRC (2011)

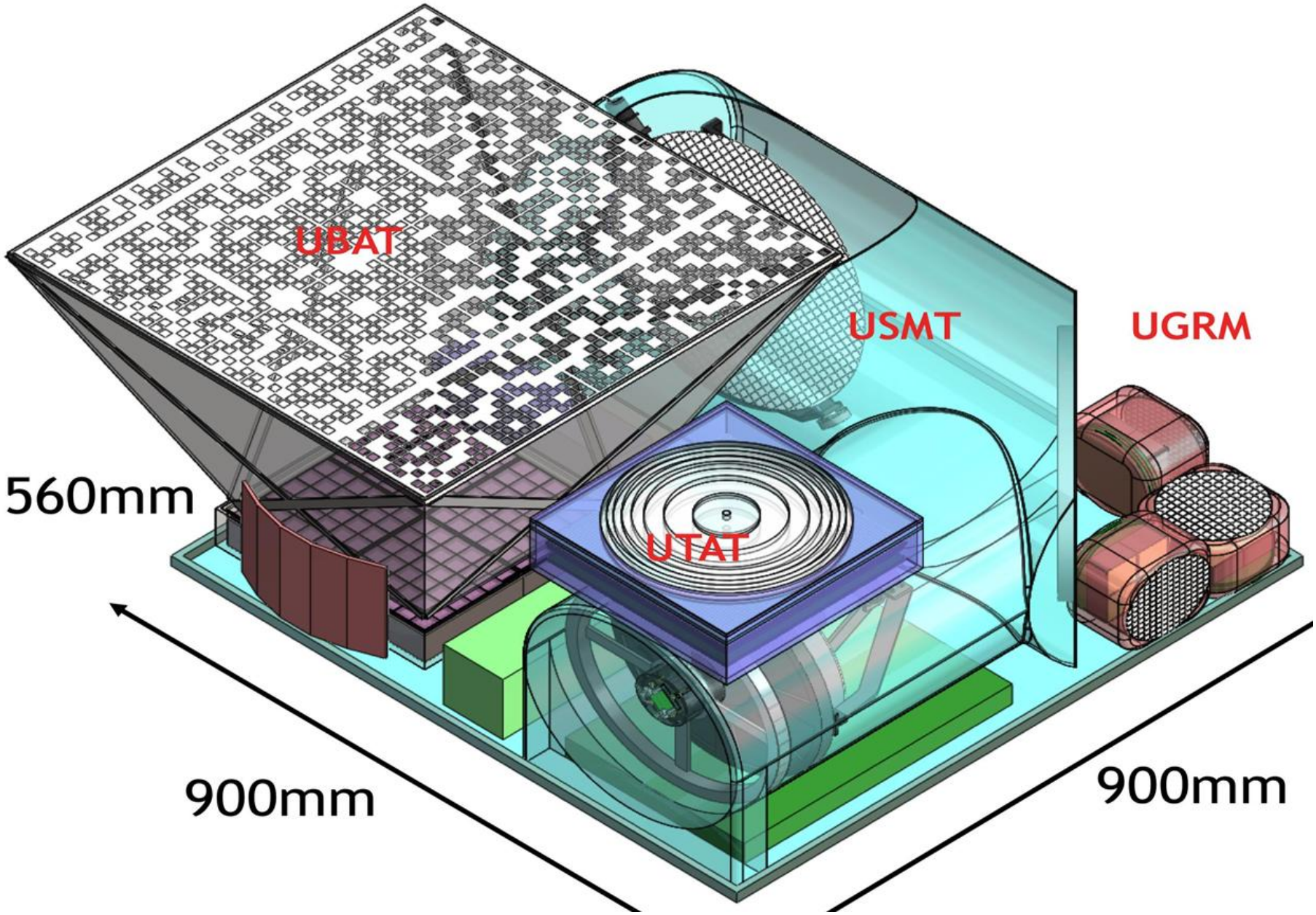

Figure 5. A rendering of the UFFO-100 GRB Telescope

P. Chen, S. Ahmad, K. Ahn, et al., 32nd ICRC (2011)

Table 2. Key parameters of UFFO Burst Alert and Trigger Telescope (UBAT).

Overall	Mass of the camera	10 kg
	Energy range	5 – 200 keV
	Telescope PSF	≤ 17 arcmin
	Source position accuracy	≤ 10 arcmin (> 7σ)
	Field of view	~1.85 sr (90.2° x 90.2°)
	GRB detection rate	~ 43/yr
Detector plane	Compounds	LYSO + MAPMT
	Effective area	191 cm^2
	Pixel size	2.88 x 2.88 x 2 mm^3
	Number of pixels	48 x 48
	Spectral energy Resolution	20% at 60 keV
	Sensitivity	310 mCrab for 10 sec exposures at 5σ, 5-100 keV
Passive shielding	Compounds (out to in)	Al, W
	Absorption @ 4-50 keV	100 %
Coded mask	Compounds	W alloy
	Total size	392 x 392 mm^2
	Mask to detector plane distance	28 cm